

Cluster Galaxies Die Hard

Simone M. Weinmann^{1*}, Guinevere Kauffmann¹, Anja von der Linden²,
Gabriella De Lucia³

¹Max-Planck Institut fuer Astrophysik, Karl-Schwarzschild-Str.1, Postfach 1317, 85741 Garching, Germany

²Kavli Institute for Particle Astrophysics and Cosmology, Stanford University, 452 Lomita Mall, Stanford, CA 94305-4085, USA

³Osservatorio Astronomico di Trieste INAF, Via Tiepolo 11, 34143 Trieste, Italy

ABSTRACT

We investigate how the specific star formation rates of galaxies of different masses depend on cluster-centric radius and on the central/satellite dichotomy in both field and cluster environments. Recent data from a variety of sources, including the cluster catalogue of von der Linden et al. are compared to the semi-analytic models of De Lucia & Blaizot. We find that these models predict too many passive satellite galaxies in clusters, too few passive central galaxies with low stellar masses, and too many passive central galaxies with high masses. We then outline a series of modifications to the model necessary to solve these problems: a) Instead of instantaneous stripping of the external gas reservoir after a galaxy becomes a satellite, the gas supply is assumed to decrease at the same rate that the surrounding halo loses mass due to tidal stripping, b) The AGN feedback efficiency is lowered to bring the fraction of massive passive centrals in better agreement with the data. We also allow for radio mode AGN feedback in satellite galaxies. c) We assume that satellite galaxies residing in host haloes with masses below $10^{12}h^{-1}M_{\odot}$ do not undergo any stripping. We highlight the fact that in low mass galaxies, the external reservoir is composed primarily of gas that has been expelled from the galactic disk by supernovae driven winds. This gas must remain available as a future reservoir for star formation, even in satellite galaxies. Finally, we present a simple recipe for the stripping of gas and dark matter in satellites that can be used in models where subhalo evolution is not followed in detail.

Key words: galaxies: cluster: general – galaxies: statistics – galaxies: haloes – galaxies: evolution

1 INTRODUCTION

It has long been known that cluster galaxies are redder, less active in their star formation, and of earlier type than galaxies in the field (e.g. Oemler 1974; Dressler 1980; Balogh et al. 1997). This difference has been found to become more pronounced towards the centers of clusters (e.g. Postman & Geller 1984; Goto et al. 2004; Barkhouse et al. 2009; Hansen et al. 2009; von der Linden et al. 2009) and perhaps also with increasing cluster mass (e.g. Weinmann et al. 2006a; Martínez et al. 2006, Kimm et al. 2009; but see also De Propriis et al. 2004 and Tanaka et al. 2004). Understanding these “environmental effects” is not only crucial for modelling the detailed properties of the global galaxy population, but it can also help us to investigate fundamental processes of galaxy evolution like star formation, supernova

feedback, feedback by active galactic nuclei, and morphological transformations. All of these processes are likely to be influenced by the decline of gas accretion in galaxies residing in group and cluster environments. Clusters and groups of galaxies thus provide unique laboratories in which we can observe the evolution of galaxies under conditions different to those in the field.

Recently, several studies have investigated the fraction of passive cluster galaxies as a function of cluster-centric radius *at fixed stellar mass*. Most of them find that an increase of the passive fraction towards the center of cluster is still detectable (Bamford et al. 2008; von der Linden et al. 2009; this work; but see also van den Bosch et al. 2008). Investigating the trends at fixed stellar mass is important since the galaxy stellar mass function may depend on environment (e.g. Balogh et al. 2001; Baldry et al. 2006; but see also von der Linden et al. 2009), and since galaxy properties are strongly correlated with stellar mass (Kauffmann et al. 2003). In this work, we determine the same relations

* E-mail:simone@MPA-Garching.MPG.DE

in the cluster catalogue of von der Linden et al. (2007), in which the brightest cluster galaxies are selected with great care and are thus likely to mark the approximate center of the cluster. This is crucial for deriving correct trends as a function of cluster-centric radius.

Semi-analytical models (hereafter referred to as SAMs, e.g. Kauffmann et al. 1993; Cole et al. 2000; Croton et al. 2006) track the evolution of galaxies over time, using simple prescriptions for the treatment of gas-physical processes combined with analytical merger trees of dark matter haloes or trees derived from N-body simulations. Most of these models treat environmental effects in a simplistic manner. Motivated by the “starvation” scenario suggested by Larson, Tinsley & Caldwell (1980), all hot gas around the satellites is immediately removed upon infall. The stripped gas is then made available for cooling to the central galaxy of the corresponding Friends-of-Friends group. This simple prescription leads to satellite galaxies that are too red (e.g. Weinmann et al. 2006b, Wang et al. 2007) compared to observations. This suggests that part of the hot gas should remain with the satellite galaxy. This is not a minor issue, since satellite galaxies constitute a significant fraction of the total galaxy population and since changing the prescription for gas stripping in satellites may have a considerable impact on the central galaxy population. First, satellites eventually merge with the central galaxies in their halo. If they can grow to higher stellar masses, central galaxies will become more massive as well. Second, if part of the hot gas stays attached to satellites, the amount of gas available for cooling to the central galaxy is reduced. Third, if satellite galaxies merging with the central galaxy still contain cold gas, the ensuing star burst will make the central galaxy bluer for a certain period of time, and will result in a higher final stellar mass.

Attempts to treat environmental effects in SAMs more realistically have already been made by Kang & van den Bosch (2008) on the basis of the Kang, Jing & Silk (2006) SAM and by Font et al. (2008), on the basis of the Bower et al. (2006) model. Kang & van den Bosch (2008) found that their simple prescription for decreasing the efficiency of gas stripping in satellites leads to a fraction of blue central galaxies which is higher than observed. They suggested counterbalancing this effect by the inclusion of an additional prescription for the disruption of satellites. Font et al. (2008) implemented a more sophisticated model based on the hydrodynamical simulations of ram-pressure stripping by McCarthy et al. (2008), and obtained better agreement with observed environmental effects than previous semi-analytic models.

Ram-pressure stripping of the cold disk gas in satellites has been studied in the SAMs of Okamoto & Nagashima (2003) and Lanzoni et al. (2005). These studies concluded that this effect has a negligible impact on the results, because the complete stripping of the hot gas halo already makes the satellites passive.

In this work, we modify the SAM of De Lucia & Blaizot (2007, hereafter DLB07) in order to reproduce (i) the relation between passive fraction and cluster-centric radius, as well as the passive fraction in field galaxies and (ii) the distribution of specific star formation rates of satellite galaxies. Up to now, this combination of observational relations has never been used to constrain SAMs (but see Diaferio et al. 2001, who study passive fractions as a function of

cluster-centric radius in a set of SAMs implemented on low-resolution N-body simulations). We apply a realistic cluster finder to the DLB07 SAM to allow for a fair comparison with observations. We find that a very simple model in which the diffuse gas halo around satellites is stripped at the same rate as the dark matter subhalo loses mass due to tidal effects gives good agreement with observations. Interestingly, we find that this stripping does not proceed exponentially, but linearly, and that this behaviour is crucial for reproducing the distribution of the specific star formation rates (SSFR) in satellites. We also implement a series of modifications to the SAM, which lead to improved agreement with the observed passive fractions as a function of stellar mass for the central galaxies. Our goal is not to obtain a full model which reproduces all the observations; rather, we look at a variety of models which allow us to understand better the complex interplay between feedback by supernovae (‘SN’ hereafter), feedback by active galactic nuclei (‘AGN’ hereafter) and satellite galaxy stripping. We also test a model in which the hot gas of satellite galaxies is removed by ram-pressure stripping, but find that this model does not reproduce observations in detail.

To summarize, the main goal of this study is to provide insight into what causes environmental effects, on which timescales they act and how they might be modelled in SAMs of galaxy formation. In section 2, we present the observational and semi-analytical data and explain the construction of our mock cluster catalogue. In section 3, we present the observational results which we use to compare to models. In section 4, we discuss the stripping of dark matter subhaloes. In section 5, we present modified versions of the SAM of DLB07, which we compare with observations in section 6. Finally, in section 7, we discuss our findings and test a model of ram-pressure stripping for comparison. In section 8, we give a summary of our results.

2 DATA

2.1 The Cluster Catalogue

We use the Cluster Catalogue of von der Linden et al. (2007, hereafter vdL07) which is based on the SDSS DR4 and the C4 Cluster Catalogue (Miller et al. 2005). The C4 Cluster Catalogue identifies clusters in a parameter space of position, redshift and colour, making use of the fact that at least a fraction of the cluster galaxies lie on a tight colour-magnitude relation. VdL07 carefully identified the brightest cluster galaxies (BCGs) in these clusters, making sure that galaxies that were not targeted spectroscopically would not be missed. They then redetermined cluster memberships and velocity dispersions using the bi-weight estimator by Beers et al. (1990), and estimated cluster masses from the velocity dispersions, as described in vdL07. Their final sample consists of 625 clusters at redshifts between 0.03 and 0.1, with masses between 10^{12} and $10^{15} h^{-1} M_{\odot}$. In most of what follows, we will focus on clusters with masses $10^{14} - 10^{15} h^{-1} M_{\odot}$ of which there are 214 in the sample. The 341 clusters with masses between $10^{13} - 10^{14} h^{-1} M_{\odot}$ will only be used for comparison. At the redshift of the most distant cluster, galaxies were observed down to a limiting magnitude of $M_r - 5 \log h = -19.75$.

In all of what follows, we weight each galaxy by the inverse of the maximum volume out to which it can be observed, given the apparent magnitude limit of the survey. Stellar masses are calculated using the method of Kauffmann et al. (2003).

2.2 Central Galaxies

In order to obtain large observational samples of central galaxies needed for comparison to the SAM, we make use of the SDSS DR4 group catalogue of Yang et al. (2007). This group catalogue has been constructed by applying the halo-based group finder of Yang et al. (2005) to the New York Value-Added Galaxy Catalogue (NYU-VAGC; see Blanton et al. 2005). From this catalogue, Yang et al. (2007) selected all galaxies in the Main Galaxy Sample with an extinction corrected apparent magnitude brighter than $m_r = 18$, with redshifts in the range $0.01 < z < 0.20$ and with a redshift completeness $C_z > 0.7$. The group catalogue is publically available and can be downloaded from <http://www.astro.umass.edu/~xhyang/Group.html>. We refer the reader to Yang et al. (2007) for a more detailed description. We only use central galaxies from this catalogue that have redshifts in the range $0.01 < z < 0.1$ in this work.

2.3 The simulation and the SAM

We use the SAM by DLB07 which is based on the Millennium Simulation (Springel et al. 2005). The SAM uses analytical prescriptions for gas accretion, gas cooling, star formation, SN feedback, AGN feedback, dynamical friction, merger-induced star bursts and reionization. These are implemented on the merger trees extracted from the Millennium Simulation, which follow dark matter haloes and subhaloes over time. Photometric properties of galaxies are computed using models for stellar population synthesis and dust. More details can be found in DLB07, Croton et al. (2006) and references therein. The SAM has been tuned to reproduce key observations like the luminosity function at $z=0$ (Croton et al. 2006; DLB07). The aspect of the SAM on which we will mainly focus in this paper is the treatment of gas in satellite galaxies, which will be explained in more detail in section 5.1. The cosmological parameters used in this model are in agreement with the WMAP1 data (Spergel et al. 2003), with $\Omega_M = 0.25$, $\Omega_\Lambda = 0.75$, $\Omega_b = 0.045$ and $\sigma_8 = 0.9$.

2.4 The SAM Cluster Catalogue

We now describe the construction of our mock cluster catalogue based on the $z=0$ output of the Millennium Simulation combined with the DLB07 SAM. Our goal is to mimic the procedure used by vdL07 to determine cluster memberships and velocity dispersions. However, we do not try to mimic the initial identification of clusters in the C4 Cluster Catalogue, or the method for identifying the brightest cluster galaxies (BCG). We make two assumptions: first, that if we impose the same magnitude limit on the cluster galaxy sample from the Millennium Run simulation as we do for the vdL07 catalogue, the resulting sample of simulated clusters can be compared directly with clusters of the same mass from our observational sample. Second, we assume that the

BCGs in vdL07 are correctly identified. The first assumption is likely not quite correct; our sample probably contains more low mass clusters than the sample of vdL07, since those are more difficult to identify observationally. The second assumption seems reasonable. VdL07, Best et al. (2007) and Koester et al. (2007) show that the BCGs of vdL07 differ systematically from other galaxies of the same mass and are good tracers of the cluster centers defined using X-ray images of the hot intracluster gas.

Clusters in the Millennium Simulation are identified with a Friends-of-Friends (FOF) algorithm (Springel et al. 2005). These FOF clusters are not necessarily spherical, but are often elongated in shape. We select the FOF clusters with $10^{13} < M_{200,\text{Mill}}/(h^{-1}M_\odot) < 10^{15}$, with $M_{200,\text{Mill}}$ the mass enclosed within a sphere with a density of 200 times the critical density of the universe. Subhaloes are identified using the SUBFIND algorithm (Springel et al. 2001). By definition, the ‘‘central galaxies’’ of clusters reside at the center of mass of the most massive subhalo in the FOF group. We use these ‘‘central galaxies’’ as starting points for determining cluster memberships and velocity dispersion, as done in vdL07 for their observational sample of BCGs.

We mimic the observational selection of vdL07 by only using galaxies with $M_r - 5\log h < -18.6$ for the construction of our mock cluster catalogues, which roughly corresponds to the absolute magnitude limit at the median redshift of the vdL07 sample. We add the Hubble flow to the z -direction of the velocities of galaxies in our simulation box, and we place all galaxies at a minimum distance of 60 Mpc from the virtual observer, so that all clusters are at least as far away as the nearest cluster in the sample of vdL07. We then follow the procedure explained in detail by vdL07, in which the bi-weight estimator of Beers et al. (1990) is applied iteratively to galaxies surrounding the cluster center, with the velocity dispersion and the cluster redshift being redetermined at each iteration step. If a galaxy belongs to more than one cluster in the final list, then we follow von der Linden et al. (2009) and only count it as a member of the one cluster for which the quantity

$$D_{\text{eff}} = \sqrt{(R/R_{200})^2 + (V/\sigma_{1D})^2} \quad (1)$$

is smaller, with

$$R^2 = (x - x_{\text{cl}})^2 + (y - y_{\text{cl}})^2 \quad (2)$$

and

$$V^2 = (v_{\text{eff,cl}} - v_{\text{eff,gal}})^2. \quad (3)$$

We only deviate from vdL07 in two ways :

- We define two cluster mass bins, one with $M_{200,\text{Mill}} = 10^{13} - 10^{14}h^{-1}M_\odot$ and one with $M_{200,\text{Mill}} = 10^{14} - 10^{15}h^{-1}M_\odot$. If a galaxy lies close to the centers of two clusters in the same mass bin, we only allow it to enter into the iterative process for the closer cluster, with the distance defined by equation 1. This prevents cluster galaxies from being falsely linked to a neighbouring cluster of similar mass. Such a step is not included in vdL07, where a given galaxy can in principle enter into the iterative process for several nearby cluster centers. We believe that this step is justified here, as the density of clusters in the simulation is higher than in an observational sample. We have checked that this constraint only increases the fraction of interlopers in the

outskirts of cluster by around 10 % and does not affect our final results.

- The initial guess for the 1D velocity dispersion is taken to be 500 km/s for all clusters. vdL07 calculate an initial guess individually for each cluster, using the average of the different velocity measurements in the C4 Cluster Catalogue. We have checked that using an initial guess of 250 km/s or 1000 km/s makes virtually no difference to our final results.

To enable faster data processing, we only use a subvolume of the Millennium Simulation, which encloses around 1/5 of the total simulation box and contains the centers of 7586 clusters with masses $10^{13} < M_{200,\text{Mill}}/(h^{-1}M_{\odot}) < 10^{15}$. We have checked that the mass distribution of these clusters is the same as in the entire simulation box. 412 clusters have a mass above $10^{14}h^{-1}M_{\odot}$. After applying our bi-weight estimator to all of the 7586 central cluster galaxies as described above, we remove all clusters which contain less than 4 members in the final iteration step, as done by vdL07. We also remove (i) all clusters which are clearly offset from the relation between velocity dispersion and number of member galaxies defined by the bulk of the cluster population and (ii) all clusters for which the position of the original BCG and the cluster center determined by the bi-weight estimator of Beers et al. (1990) differ by more than 0.002 in redshift. This step is necessary since such clusters have undergone special treatment in vdL07, which we do not repeat here. It affects less than 3 % of the clusters in our sample. Finally, we are left with 4393 clusters, constituting what will be called the “Beers-Millennium Cluster Catalogue” in what follows. The reason for the high reduction in sample size going from the Millennium Cluster Catalogue to the Beers-Millennium Catalogue is simply that our initial Millennium Cluster sample contains many relatively low mass clusters, of which many contain less than four galaxies. The 1D velocity dispersion of clusters with a low number of member galaxies also has a large scatter, which makes convergence of the bi-weight estimator of Beers et al. (1990) less likely.

We estimate M_{200} for the clusters in our final sample from the 1D velocity dispersions according to eq. 1 of vdL07. In all of what follows, M_{200} or the “cluster mass” refers to the mass as obtained in this way. 3151 of the clusters in the “Beers-Millennium Cluster Catalogue” are assigned a mass above $10^{13}h^{-1}M_{\odot}$, 747 above $10^{14}h^{-1}M_{\odot}$. We therefore have significantly more galaxies with masses above $10^{14}h^{-1}M_{\odot}$ than in our initial Millennium Cluster Catalogue. This already indicates that a non-negligible number of clusters have masses that are overestimated.

We now compare the properties of the Millennium Cluster Catalogue catalogue and the Beers-Millennium Cluster Catalogue in detail. In the top panel of Fig. 1, we show the distribution of halo masses in the three catalogues used in this work: The vdL07 cluster catalogue, the original Millennium cluster catalogue and the recovered Beers-Millennium catalogue. The original distribution of halo masses is clearly smeared out for the clusters in the recovered Beers-Millennium catalogue. In the bottom panel of Fig. 1, we show the scatter between the true and recovered halo masses in the Beers-Millennium catalogue. The scatter is large because of the considerable loss of information that occurs when going from the 3-dimensional to the

1-dimensional velocity dispersion. This effect is especially severe for low mass clusters which have only a low number of detectable members. This means that that a large fraction of the massive Beers-Millennium Clusters, on which we focus our analysis, have their masses and radii overestimated, i.e. are low mass clusters in the Millennium Catalogue. Consequently, the galaxy population in the cluster outskirts will be strongly contaminated by interlopers.

We now examine the interloper fraction in our clusters in more detail. Any galaxy which is identified as a member of a Beers-Millennium cluster by the bi-weight algorithm, but does not actually reside within $R_{200,\text{Mill}}$ of the corresponding true Millennium cluster, is defined as an interloper. In Fig. 2, we show the interloper fractions as a function of cluster-centric radius for clusters with $M_{200} = 10^{14} - 10^{15}h^{-1}M_{\odot}$. The cluster center is defined to lie at the position of the central cluster galaxy. The interloper fraction in the center is very low, but rises steeply towards the outskirts, as expected. Since we have used a similar method as vdL07, our finding indicates that a similar contamination might be present in their study¹. Dashed lines show the fraction of interlopers which are central galaxies in the Millennium Catalogue. This fraction is very small, showing that most of the interlopers are in fact satellite galaxies; they either belong to the extended filaments surrounding the cluster (and are as such part of the FOF cluster), or are part of infalling nearby groups. Note that as many as 40% of all satellite galaxies in the SAM actually reside beyond $R_{200,\text{Mill}}$ of their respective central galaxy. These interlopers have by definition experienced environmental effects in the SAM and cannot be considered true “contamination” from the field; however, the time at which they fell into the cluster will differ from galaxies that reside within R_{200} of the cluster center.

We conclude that there is a high interloper fraction in clusters identified with a typical cluster-finding algorithm, and a relatively large scatter between true and recovered mass. This means that it is crucial to mimic the observational cluster finding process when examining environmental effects in models.

3 OBSERVATIONS

3.1 Defining passive and active galaxies

We use the specific star formation rate (SSFR) to distinguish passive and active galaxies. The reason for our choice is that the SSFR is a physical quantity with a straightforward meaning. It can be directly taken from the SAM without any assumptions about stellar population synthesis models. However, the SSFR is not a directly observed quantity.

Brinchmann et al. (2003) have derived SSFRs for galaxies in the SDSS using emission lines, the D4000 spectral index and colours, with colours used for sampling star formation outside the region covered by the fiber. Salim et al. (2007) have redetermined SSFRs for a subset of these galaxies from UV and optical photometry, and while they find

¹ It is however likely that the sample of vdL07 is biased towards higher cluster masses, since these are observationally easier to detect, which could make our contamination slightly higher than in vdL07.

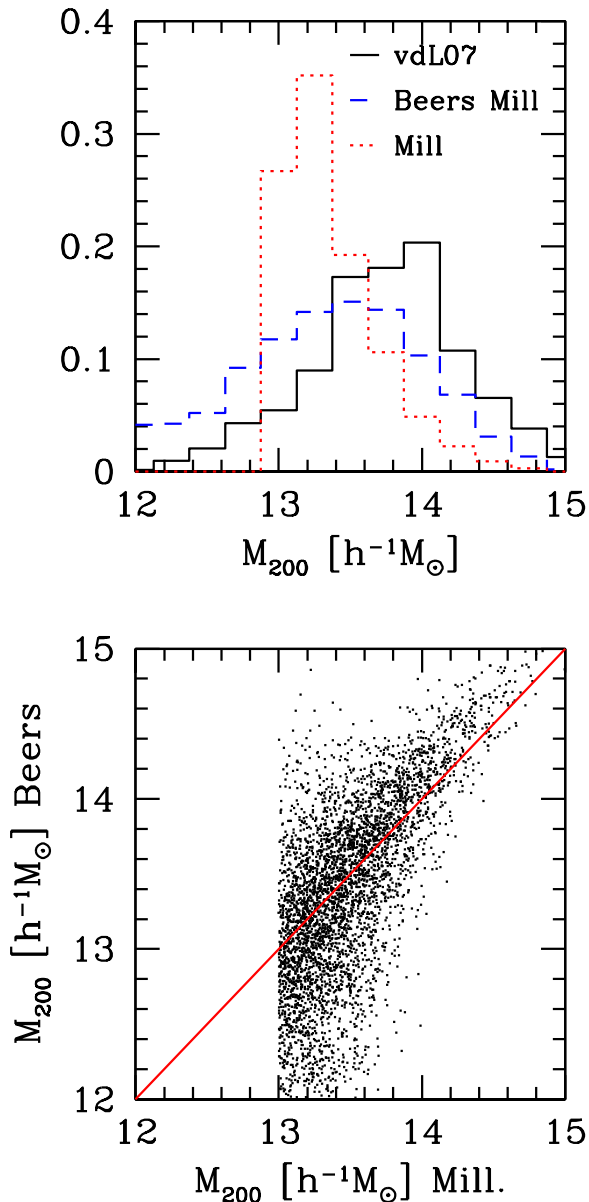


Figure 1. Top panel: The fractional distribution of cluster masses for the 625 clusters in the vdL07 catalogue (black line) for the 4393 clusters in the Beers-Millennium-Catalogue (blue dashed line) and for the 7586 clusters in the Millennium Catalogue (red dotted lines). Bottom panel: The relation between true and recovered halo masses for the 4393 clusters in the Beers-Millennium Catalogue. Clusters with masses around $10^{13} h^{-1} M_{\odot}$ in the Millennium Catalogue suffer from a particularly large scatter in the halo mass, due to their low number of member galaxies which causes a large spread in 1D velocity dispersion.

good agreement for the “star-forming” class of the Brinchmann et al. (2003) sample, they also find that star formation rates are overestimated for the “star forming low S/N”, the “Composite”, the “AGN” class and the galaxies without measured $H\alpha$ (see Salim et al. 2007 and Schiminovich et al. 2007 for more details). We therefore decide to use the SSFR from Brinchmann et al. (2003), but with a rough correction, bringing it into statistical agreement with Salim et al. (2007). For “low S/N” galaxies, “AGN” and “composite”

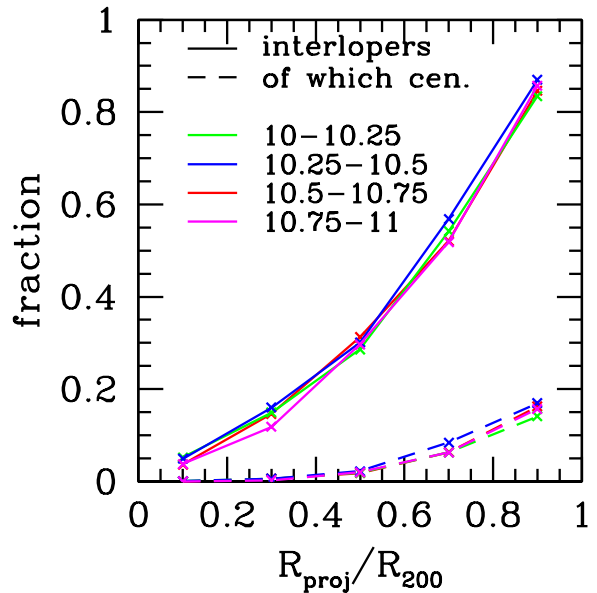


Figure 2. Fraction of interlopers (i.e. galaxies that reside outside R_{200} in the Millennium Catalogue) in the Beers-Millennium clusters with masses $10^{14} - 10^{15} h^{-1} M_{\odot}$, in four different logarithmic stellar mass bins, as indicated. Note that the definition of an interloper used here is very strict and many galaxies classified as interlopers actually belong to the (non-spherical) large-scale structure associated with the cluster. Dashed lines show the fraction of interloper galaxies which are centrals in the Millennium Catalogue.

galaxies, and galaxies with no $H\alpha$, we scale the Brinchmann et al. (2003) star formation rates down by 0.2, 0.4 and 1.0 dex to correct for the offsets seen in Fig. 3 of Salim et al. (2007). The SSFR for the “star-forming” galaxies are used without any correction.

In Fig. 3, top panel, we show the SSFR as a function of stellar mass for central galaxies in the SAM. A very clear star forming sequence at around $\log(\text{SSFR}) = -10$ can be seen. In the bottom panel of the same figure, we show the corrected SSFR for central galaxies in the SDSS. These were determined using the Yang et al. (2007) group catalogue and not vdL07, since it also includes low mass groups and thus provides much better statistics. Every galaxy is weighted by $1/V_{\text{max}}$, where V_{max} is the maximum volume out to which a galaxy of that magnitude would be detected in the survey. We define “passive galaxies” as those with $\log(\text{SSFR}) < -11$ both in the SAM and in the SDSS, because this cut corresponds roughly to the location of the minimum in the bimodal distribution of SSFR in both the model and the observations.

Comparing the overall distributions in the SDSS and the SAM, we see that the shape of the star forming sequence is tilted in the SDSS, unlike in the SAM. This problem has been noted before (e.g. Somerville et al. 2008), and seems to be generic to current SAMs (but see Neistein & Weinmann 2009)

3.2 Observational Results

Here, we present the observational results that will be used as the basis for our model comparisons in what follows.

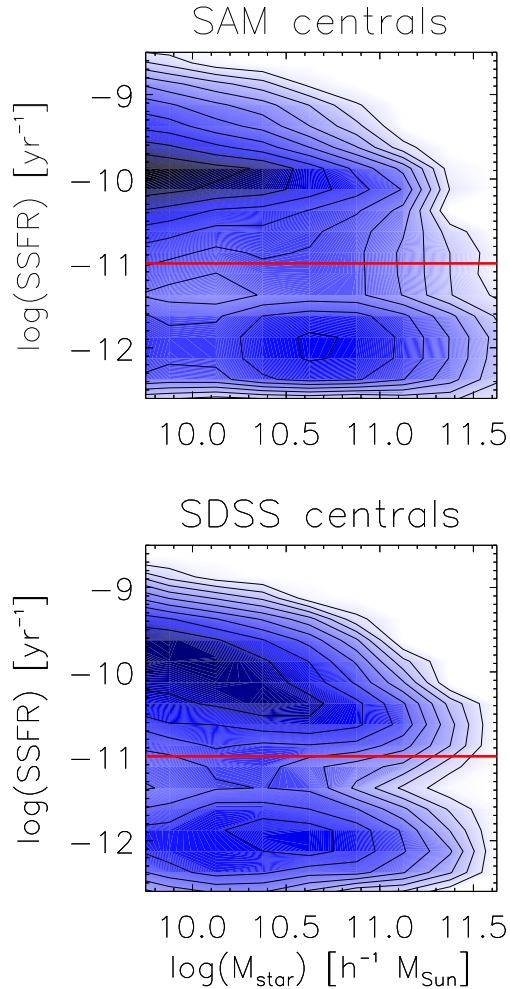


Figure 3. The SSFR as a function stellar mass in the SAM and the SDSS, for central galaxies only. Red lines indicate how we divide galaxies into “passive” and “active” in all of what follows. In the SDSS, we use the Brinchmann et al. (2003) SSFRs, corrected such that the offset with respect to Salim et al. (2007) is removed. In the SAM, galaxies with zero star formation rate have been randomly assigned SSFRs between -11.6 and -12.4 , and the same has been done for SDSS galaxies which have measured SSFRs, but with values < -12.4 , since such low SSFRs tend to have large errors. In the SDSS, only galaxies with $z < 0.1$ are used, and a V_{max} -correction has been applied. The number of galaxies has been normalized to the same value in both panels.

These include the passive fraction of central galaxies as a function of stellar mass, the fraction of passive galaxies as a function of cluster-centric radius, and the distribution in SSFR for satellite and central galaxies. For all observations, we apply volume-weighting to correct for the apparent magnitude limit of the SDSS.

In our Fig. 8, we show as crosses with errorbars the passive fraction of central galaxies as a function of stellar mass defined using the group catalogue of Yang et al. (2007). As we show in Neistein & Weinmann (2009), similar results are obtained if the SSFRs of Salim et al. (2007) are used directly.

We use the cluster catalogue of vdL07 to determine

passive fractions as a function of projected cluster-centric radius in the SDSS (crosses with errorbars in Fig. 9). All galaxies within $3 \cdot \sigma_{1D}$ of the cluster center are used in this plot. Errorbars are determined using jackknife resampling. We have checked that results are virtually unchanged if we define volume-limited samples that are complete down to a given limiting stellar mass, as done by von der Linden et al. (2009). For the three lower stellar mass bins, the passive fractions as a function of cluster-centric radius are nearly identical to what has been found by von der Linden et al. (2009), which is somewhat surprising, since they have defined passive galaxies completely differently, with a method based on the light-weighted age of the stellar population, rather than the current SSFR as done here. This indicates that our way of classifying galaxies into passive and active is robust, at least at masses below $\log(M/h^{-1}M_{\odot})=10.75$. At higher masses, passive fractions are systematically lower by 10-15 % than in von der Linden et al. (2009).

In Fig. 10 and Fig. 11 we show as black histograms the distribution of SSFRs for SDSS central galaxies as defined by Yang et al. (2007), and for satellite galaxies defined here as galaxies located at a distance of less than R_{200} and within $3 \cdot \sigma_{1D}$ from the center of a cluster with mass $\log(M/h^{-1}M_{\odot}) > 14$ in the catalogue of vdL07. A clear bimodality can be seen for both galaxy populations.

4 DARK MATTER EVOLUTION OF SUBHALOES

In this section, we investigate the stripping of dark matter subhaloes in the Millennium simulation. Stripping of subhaloes has been studied numerically e.g. by Hayashi et al. (2003); Gao et al. (2004); De Lucia et al. (2004); Kazantzidis et al. (2004); Zentner et al. (2005); Giocoli et al. (2008); Diemand, Kuhlen & Madau (2007) and observationally using weak gravitational lensing signals e.g. by Limousin et al. (2007) or Natarajan et al. (2009). The results presented here will be important for the new prescriptions for satellite evolution that will be introduced in the next section.

In Fig. 4, we show the median fraction of dark matter which has been stripped since infall, for satellite galaxies in clusters and groups at $z=0$ (left hand and middle panel) and at $z=1$ (right hand panels), as a function of lookback time to infall. We have checked that results do not strongly depend on host halo mass down to $10^{12}h^{-1}M_{\odot}$. Different linestyles denote different bins of M_{infall} . Satellite galaxies are defined as galaxies which are part of a FOF group, but are not the central galaxy of the most massive subhalo. For the satellite galaxies at $z=0$, we adopt two different methods for treating subhaloes which fall below the resolution limit (sometimes called “orphan galaxies”). In the left hand panel, we assume that their mass falls instantaneously to zero, while in the middle panels, we set the mass equal to the effective resolution limit. For the highest mass subhaloes, the results are little affected by resolution and the curves in the left and middle panel are similar. For low mass subhalos, the two prescriptions (not surprisingly) give quite different results. The plots indicate that the Millennium simulation can be used to follow subhalo evolution to high accuracy for systems where M_{infall} is larger than $10^{11}h^{-1}M_{\odot}$.

Our results for such subhalos indicate that the dark

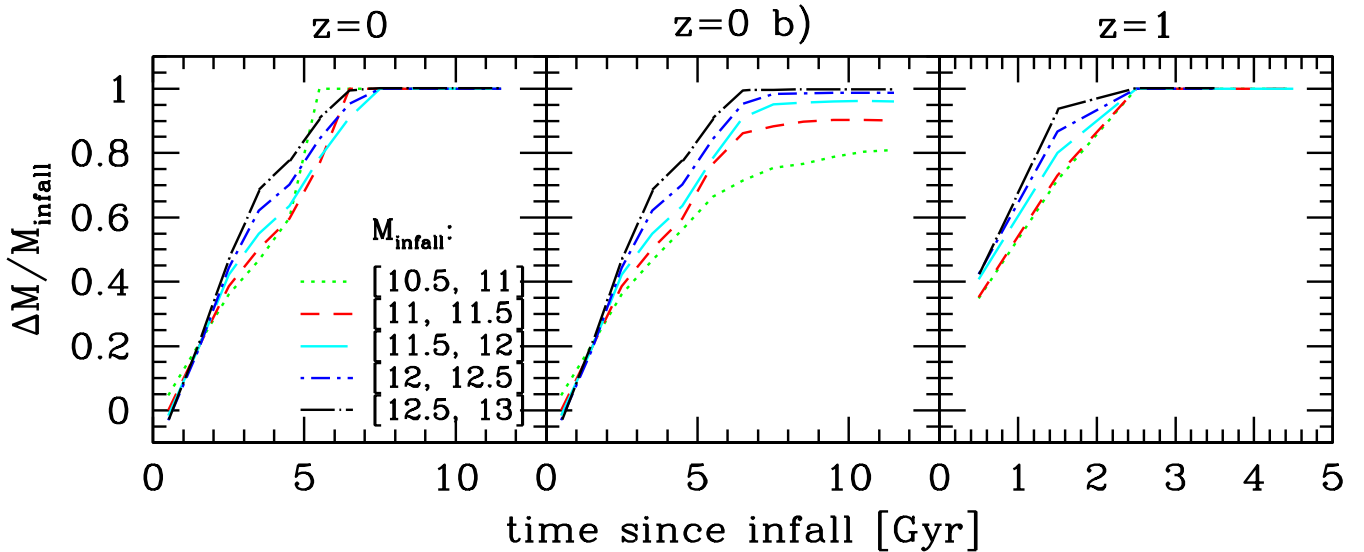


Figure 4. The median fraction of subhalo mass which has been stripped since infall as a function of the lookback time to infall. Only subhaloes containing galaxies with masses $> 10^{9.5} h^{-1} M_{\odot}$ today in DLB07 are used. In the left hand panel, we show results for satellites at $z=0$ if the mass of unresolved subhaloes is set to zero. In the middle panel, we show results for satellites at $z=0$ if the mass of unresolved subhaloes is set to the resolution limit of $1.7 \times 10^{10} h^{-1} M_{\odot}$, for illustration. In the right hand panel, we show results for $z=1$, with the mass of unresolved subhaloes set to zero.

matter is usually nearly completely stripped after the subhalo has spent 5-7 Gyr in the cluster. Interestingly, we find that stripping is surprisingly similar for subhaloes spanning two orders of magnitude in dark matter mass at infall, if the dark matter mass of orphan galaxies is set to zero. We find that for satellite galaxies identified at $z=0$, roughly 15-20 % of the initial dark matter mass has been stripped per Gyr elapsed since infall. Note that the decline is not exponential. This means that *stripping becomes more efficient the longer a subhalo has been a satellite*. This can be explained by the fact that subhaloes which have already spent a significant amount of time as satellites have sunk to the center of the potential well (Gao et al. 2004), where stripping becomes fast, while a large fraction of subhaloes just having fallen in recently will be at the outskirts of the FOF group where stripping is inefficient. Note that the stripping for an *individual* subhalo typically proceeds much less smoothly than the median shown here, as a large fraction of the stripping occurs at the first pericenter passage (e.g. Diemand et al. 2007).

For galaxies which are satellites at $z=1$ (right hand panel of Fig. 4), the dark matter stripping since infall has been significantly more efficient, with ~ 40 % of the initial dark matter mass stripped per Gyr in the median. This indicates that the stripping efficiency increases towards higher redshift, which is expected due to the decrease of dynamical times. This result is in qualitative agreement with the findings of Giocoli et al. (2008) and Tinker & Wetzel (2009). Note that both Natarajan, De Lucia & Springel (2007) and Maciejewski et al. (2009) have found indications that the subhalo masses found with SUBFIND are systematically low with respect to the true mass enhancement, or the masses found with more accurate 6D substructure finders. This effect is most severe in the inner regions of clusters, where the background density of the parent cluster is high (Natarajan et al. 2007). This means that our estimates of dark matter

stripping might be slightly too high, especially for subhaloes close to the cluster center. An alternative, and perhaps more accurate, method for estimating the amount of stripping in subhaloes would be to combine SAMs with analytical prescriptions based on higher resolution dark matter simulations, like presented in Taylor & Babul (2001).

5 THE MODELS

In this section, we present both the standard SAM of DLB07 and our modifications of this model.

5.1 The standard model

Here we give an overview of how gas physics is modelled in central and satellite galaxies in DLB07 and repeat the basic equations (as given and explained in more detail in Croton et al. 2006 and references therein) for clarity.

For central galaxies, gas surrounding galaxies comes in three phases: The cold gas, the hot gas and the ejected gas. Gas accreting onto the galaxy from the IGM is added to the hot phase. From this reservoir, it can cool down to the cold phase. Cooling is assumed to proceed differently in the “hot halo regime” (where $r_{\text{cool}} < R_{\text{vir}}$) than in the “rapid cooling regime” (where $r_{\text{cool}} > R_{\text{vir}}$). In the hot halo regime, cooling rates are given by

$$\dot{m}_{\text{cool}} = 0.5 m_{\text{hot}} \frac{r_{\text{cool}} V_{\text{vir}}}{R_{\text{vir}}^2}. \quad (4)$$

R_{vir} is the virial radius of the dark matter halo, V_{vir} the virial velocity and r_{cool} is the radius where the local cooling time t_{cool} is equal to the halo dynamical time. The local cooling time is given by

$$t_{\text{cool}} = \frac{3}{2} \frac{m_p k T}{\rho_g(r) \Lambda(T, Z)} \quad (5)$$

with m_p the mean particle mass, k the Boltzmann constant, and $\Lambda(T, Z)$ the cooling function according to Sutherland & Dopita (1993) as a function of the temperature of the gas, which is assumed to be equal to the virial temperature of the halo, and the gas metallicity. $\rho_g(r)$ is the hot gas density, which is assumed to have an isothermal profile

$$\rho_g(r) = \frac{m_{\text{hot}}}{4\pi R_{\text{vir}} r^2}. \quad (6)$$

If $r_{\text{cool}} > R_{\text{vir}}$, the cooling rate is set roughly to the rate at which new diffuse gas is added to the halo (see discussion in Croton et al. 2006).

The energy input due to radio mode AGN feedback according to Croton et al. (2006) is assumed to partially offset the cooling in high mass haloes, giving rise to a modified cooling rate

$$\dot{m}_{\text{cool,mod}} = \dot{m}_{\text{cool}} - \frac{L_{\text{BH}}}{0.5V_{\text{vir}}^2} \quad (7)$$

with the mechanical heating energy generated by the black hole accretion L_{BH} given by

$$L_{\text{BH}} = \eta \dot{m}_{\text{BH}} c^2. \quad (8)$$

$\eta=0.1$ is the standard efficiency with which mass is assumed to produce energy near the event horizon, and c the speed of light. The quiescent growth rate of the black hole is given by

$$\dot{m}_{\text{BH}} = \kappa_{\text{AGN}} \left(\frac{m_{\text{BH}}}{10^8 M_{\odot}} \right) \left(\frac{f_{\text{hot}}}{0.1} \right) \left(\frac{V_{\text{vir}}}{200 \text{ km s}^{-1}} \right)^3 \quad (9)$$

where m_{BH} is the black hole mass, f_{hot} the fraction of the total halo mass in the form of hot gas and κ_{AGN} a free parameter set to $7.5 \cdot 10^{-6} M_{\odot} \text{ yr}^{-1}$ in DLB07.

The cold gas then forms stars according to

$$\dot{m}_{\text{star}} = \alpha_{\text{SF}} (m_{\text{cold}} - m_{\text{crit}}) / t_{\text{dyn,disk}} \quad (10)$$

with $t_{\text{dyn,disk}} = r_{\text{disk}} / V_{\text{vir}}$, $r_{\text{disk}} = 3(\lambda/\sqrt{2})R_{\text{vir}}$ (motivated by the studies of Mo et al. 1998 and van den Bergh et al. 2000), and λ the spin parameter of the dark matter halo in which the galaxy resides. α_{SF} is a tunable parameter and set to 0.03 in DLB07. The calculation of the critical gas mass follows Kauffmann (1996) and is based on the observations of Kennicutt (1998) of a threshold gas density below which stars do not form anymore:

$$m_{\text{crit}} = 3.8 \cdot 10^9 \left(\frac{V_{\text{vir}}}{200 \text{ km s}^{-1}} \right) \left(\frac{r_{\text{disk}}}{10 \text{ kpc}} \right) M_{\odot}. \quad (11)$$

Supernova feedback heats cold gas back to the hot phase with an efficiency directly proportional to the star formation rate:

$$\Delta m_{\text{hot}} = \epsilon_{\text{disk}} \cdot \Delta m_* \quad (12)$$

based on the observations by Martin (1999), with $\epsilon_{\text{disk}} = 3.5$ set by observational data. Gas in the hot phase can be transported to the ejected phase due to the excess energy present in the hot halo after reheating, with an efficiency inversely proportional to the depth of the dark matter halo potential:

$$\Delta m_{\text{ejected}} = \left(\epsilon_{\text{halo}} \frac{V_{\text{SN}}^2}{V_{\text{vir}}^2} - \epsilon_{\text{disk}} \right) \Delta m_* \quad (13)$$

with $V_{\text{SN}}=630 \text{ km s}^{-1}$ the mean energy in supernova ejecta per unit mass of stars formed, based on a standard IMF and

standard supernova theory, and $\epsilon_{\text{halo}}=0.35$ tuned to reproduce observations. Per halo dynamical time, half of the gas in the ejected phase is assumed to be reaccreted to the hot phase:

$$\Delta m_{\text{ejected}} = -\gamma \cdot m_{\text{ejected}} / t_{\text{dyn}} \quad (14)$$

with $\gamma=0.5$ and t_{dyn} the halo dynamical time.

In Fig. 5, we plot the fraction of the total gas in the cold, hot and ejected phase in central galaxies at $z=0$ both as a function of galaxy stellar mass and of dark matter halo mass in the DLB07 SAM. Clearly, the ejected phase strongly dominates both at low stellar and halo masses, where the hot phase is relatively unimportant. This is a consequence of the rapid cooling and the very efficient SN feedback in low mass haloes, and indicates that the ejected phase, and how it is reaccreted, is of crucial importance for the evolution of low mass galaxies (see also Oppenheimer et al. 2009).

Satellite galaxies in DLB07 are defined as all galaxies which are member of FOF groups, but not the central galaxy of the most massive subhalo. In all our models presented below, we will follow this definition. If a galaxy becomes a satellite in DLB07, both the hot and ejected gas is removed. Any hot and ejected gas produced after infall is stripped as well. Due to the strong efficiency of SN feedback in the model, this leads to a quick depletion of cold gas and to the cessation of star formation. All stripped satellite gas is added to the hot gas of the central galaxy.

5.2 Changes to the standard model

In what follows, we describe our basic changes to the standard DLB07, which are ingredients of all our models 1) - 4) described below.

- We allow cooling from the hot to the cold gas, and reincorporation from the ejected to the hot gas, for satellite galaxies. More details are given below.

- In the DLB07 SAM, processes like cooling and star formation in galaxies are correlated with the properties of the corresponding halo, as apparent from the equations given above. After a galaxy becomes a satellite, this is not necessarily appropriate. For example, it might not generally be true that the disk radius of a satellite decreases in proportion to the radius of its dark matter halo, as assumed in DLB07. De Lucia & Helmi (2008) therefore fix the disk radius of the satellite at infall. It is also unclear how the hot gas halo redistributes itself after part of the dark matter has been stripped. In our modified model, we fix R_{vir} , λ and V_{vir} for satellites in eq. 4-14 at infall and do not let it evolve anymore. This means that star formation, cooling, ejection and reincorporation for satellites are calculated according to the subhalo properties at infall. We still follow the true evolution of the dark matter subhalo in detail, as it is used for (i) determining dynamical friction timescales and (ii) our new recipes for satellite stripping, as described below.

- Unlike DLB07, we allow AGN feedback for satellite galaxies as described in eq. 7, 8 and 9 in our models 1) - 4), again using R_{vir} and V_{vir} as determined at infall. As radio AGN activity has been observed in satellite galaxies (e.g. Best et al. 2007; Pasquali et al. 2009a), this step seems well justified.

- It has been found in previous work (e.g. Weinmann et

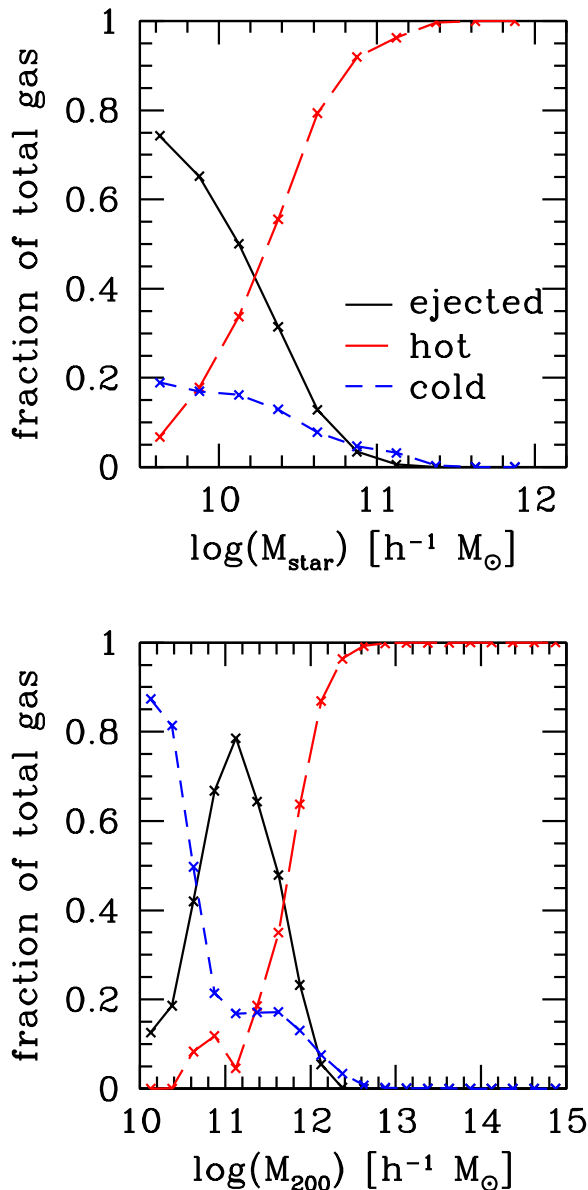


Figure 5. The average fraction of gas in the cold, hot and ejected phase, at $z=0$, as a function of stellar mass (top panel) and of halo mass (bottom panel), for central galaxies with stellar masses above $\log(M/h^{-1}M_{\odot})=9.5$ in the SAM of DLB07.

al. 2006b) that satellite galaxies in DLB07 are too red. As mentioned before, DLB07 assumes that all hot and ejected gas is removed from satellites. We find that letting satellite galaxies keep their entire hot gas, while completely stripping the ejected phase, still produces too many passive low mass satellites, as only a small fraction of the gas in these galaxies is actually in the hot mode (see Fig. 5). We therefore use a different approach. At each timestep, we assume that some fraction f_{strip} of $M_{\text{diffuse}} = M_{\text{hot}} + M_{\text{ejected}}$ is stripped. We assume that the ejected gas is always stripped first, which means that the hot gas reservoir is only stripped when $f_{\text{strip}} \cdot M_{\text{diffuse}} > M_{\text{ejected}}$. All the stripped gas is always added to the hot gas of the central galaxy in the corresponding FOF group. In our models 1) - 3), we strip the diffuse gas halo of satellite galaxies in proportion to the dark matter

subhalo. This means that if a given satellite galaxy loses a fraction of its dark matter mass between two subsequent timesteps $i-1$ and i , the same fraction $f_{\text{strip},i}$ of the current mass in diffuse gas is removed.

$$f_{\text{strip},i} = 1 - \frac{M_{\text{DM},i}}{M_{\text{DM},i-1}} \quad (15)$$

To calculate cooling rates, we need to make an assumption about the hot gas density profile of satellites. Here we simply assume that the remaining hot gas redistributes itself according to eq. 6 (with R_{vir} as recorded at infall) after each stripping event. This means that the gas becomes progressively more diluted, which additionally decreases cooling rates. This method differs from Font et al. (2008), who determine a stripping radius and remove all gas outside of this radius, causing the hot gas halo to become increasingly compact. We think that our simpler approach is justified, because the distribution of the hot gas in satellite galaxies is highly uncertain; continued energy input by SN feedback might well cause the hot gas halo to expand after a stripping event has occurred. Also, it is not entirely clear how R_{vir} and V_{vir} should be calculated for subhaloes.

Finally, we note that if the satellite galaxy falls below the resolution limit, all the hot and ejected gas is stripped at the timestep of transition. After that, the gas content of the galaxy only evolves as a result of star formation and SN feedback.

5.3 Specific Modifications

We carry out a series of progressive modifications to the semi-analytic models of DLB07, denoted modifications 0) - 3), as described below. We also try out a simpler approach, which does not follow the stripping of the DM haloes in detail, denoted modification 4).

- In our modification 0), the only change with respect to DLB07 is that we use R_{vir} and V_{vir} as recorded at infall in eq. 4-14, as described in section 5.2, second point. Since all hot and ejected gas is still removed from satellites, cooling and reincorporation rates for satellites are still zero, as in DLB07. We have checked that results are virtually indistinguishable from DLB07, with the only exception of satellite morphologies, which are brought into better agreement with observations. We plan to study this issue in future work.

- In our modification 1), we implement all the changes described in section 5.2, i.e. we strip the diffuse gas in proportion to the dark matter.

- For modification 2), we additionally decrease the quiescent hot gas accretion rate to the black hole κ_{AGN} (as defined in eq. 9) by a factor of 5, and we let satellite galaxies residing in host haloes with masses below $10^{12}h^{-1}M_{\odot}$ keep all their hot and ejected gas. The motivation for this is discussed in section 6.3. For illustration, we also present a modification 2b), which only includes the decrease in κ_{AGN} .

- While the dark matter subhalo mass for most simulated satellite galaxies continuously decreases, there are also cases in which a subhalo seems to experience dark matter growth. The reason for this is mainly that the SUBFIND algorithm (Springel et al. 2001), which is used to identify subhaloes, defines the boundary of a subhalo as the point where the density is equal to the background density. The same sub-

halo will therefore have a lower mass assigned if it is close to the center of its host halo, compared to when it is residing in the outskirts. This can lead to artificial mass fluctuations and thus to overstripping of diffuse gas in our approach. We correct for this effect in our modification 3). If the dark matter subhalo mass at a given timestep is higher than in the previous timestep, we add the appropriate amount of gas to the hot gas halo of the satellite.

- Modification 4) differs from the previous ones, since it does not rely on following the stripping of dark matter subhaloes. This prescription may be used by SAMs which do not follow the stripping and the orbits of subhaloes after they have become part of a FOF group (like e.g. Somerville et al. 2008). We simply store the mass in diffuse gas at the time of infall, and strip some fixed fraction of this initial (not the current!) diffuse gas mass per Gyr. We determine this fraction by tuning the model to fit observations. We also require that the median stripped dark matter fraction roughly agrees with the results calculated directly from the simulations, which have been discussed in section 4. We find that a good solution is to strip 20 % of the initial gas mass per Gyr if the subhalo mass at infall is $< 5 \times 10^{11} h^{-1} M_{\odot}$, and 10 % per Gyr if it is above this mass. As in our models 2) and 3), we decrease the AGN feedback efficiency, satellites residing in groups with masses below $10^{12} h^{-1} M_{\odot}$ are not stripped at all, and as in models 1) - 3), we always first strip the ejected, and then the hot gas.

A summary of our models is given in Table 1.

6 RESULTS

In this section, we compare the model results to the observational results described in section 3.2. For all plots in this section, we use the same subvolume of the Millennium Simulation as used in section 2.4. The bi-weight algorithm described in the same section is re-applied for each new model. For the model results shown in the plots in this section, central galaxies are defined as the galaxy belonging to the most massive subhalo in a given FOF group, while satellites are defined to be those galaxies located at a projected distance of less than R_{200} and within $3 \cdot \sigma_{1D}$ from the center of a cluster with $\log(M/h^{-1} M_{\odot}) > 14$ (with M determined using the bi-weight algorithm).

6.1 Modification 0

Implementing modification 0) gives results that are virtually indistinguishable from DLB07. In Fig. 8, we compare the passive fraction of central galaxies in modification 0) (blue dotted line) with observations (data points). Surprisingly, the agreement is rather poor. At intermediate stellar masses, the passive fraction is underproduced, while it is overproduced at high stellar masses. The disagreement at intermediate stellar masses might partially be due to the contamination of the central galaxy sample of Yang et al. (2007) by satellite galaxies². However, it is more likely that

² The fraction of galaxies which are satellites at masses $\log(M_{\text{star}}/h^{-1} M_{\odot}) \sim 10$ is higher by $\sim 15\%$ in the SAM than in Yang et al. (2007). Under the rather extreme assump-

Table 1. Overview of the five modified version of DLB07 discussed in this paper. Modifications 1) - 4) include all the changes discussed in section 5.2, modification 0) only the first point. κ_{AGN} is the quiescent hot gas accretion rate to the black hole in M_{\odot}/yr , as defined in Croton et al. (2006). For modification 4), f_1 and f_2 are the fractions of the initial diffuse gas stripped per Gyr. f_1 is for an initial subhalo mass of $< 5 \cdot 10^{11} h^{-1} M_{\odot}$, f_2 for higher masses.

	κ_{AGN}	sat. stripping	line
0)	$7.5 \cdot 10^{-6}$	instantaneous	blue dotted
1)	$7.5 \cdot 10^{-6}$	$\propto \text{DM}$	cyan solid
2)	$1.5 \cdot 10^{-6}$	$\propto \text{DM} > 10^{12} h^{-1} M_{\odot}$	green long-dashed
3)	$1.5 \cdot 10^{-6}$	as 2) + accretion	red dashed
4)	$1.5 \cdot 10^{-6}$	$f_1=0.2, f_2=0.1$	magenta dot-dashed

DLB07 underproduces the number of passive central galaxies at intermediate masses. This problem has already been noted by Baldry et al. (2006) and Bolzanella et al. (2009) who found that Croton et al. (2006) model did not produce enough blue central/field galaxies. The apparent overproduction of passive galaxies with low SSFR at high stellar masses, on the other hand, is more puzzling, since the fraction of *red*, massive galaxies seems to be in agreement with observations (e.g. Weinmann et al. 2006b). There are two potential explanations for this apparent discrepancy. First, precise determination the SSFRs of massive, red galaxies is difficult, and it is entirely possible that they may have been overestimated in our data. We note that von der Linden et al. (2009) find higher passive fractions at $\log(M_{\text{star}}/h^{-1} M_{\odot}) \sim 10.7$ than we do here. Second, it is important to remember that passive fractions defined according to colour are different from those defined according to SSFRs. Colours are sensitive to dust attenuation as well as the fraction of young stars in the galaxy, so the agreement with the fraction of red objects found in previous work (e.g. Croton et al. 2006) may just have been fortuitous. The main goal of the current paper is to improve the treatment of environmental effects, so we will not investigate this issue in detail; we simply decrease AGN feedback in some of our models, as described below.

In Fig. 9, we compare modification 0) (blue dotted line) with the passive fractions as a function of cluster-centric radius. Clearly, the model overproduces passive satellites, in agreement with previous findings (e.g. Weinmann et al. 2006b). In Fig. 10 and Fig. 11, we show the distribution of SSFR for central and satellite galaxies in modification 0) (blue lines) compared to observations (black lines). The number of satellite galaxies with high star formation rates is clearly too low compared to the observations. For the central galaxies, the location of the active peak is not correctly reproduced, as a result of the missing tilt in the relation between SSFR and stellar mass discussed before. For all models discussed below, the location of the two peaks for the central

tions that the satellite fraction in the SAM is correct, that these additional 15 % of satellites are wrongly counted as centrals in the Yang et al. (2007) group catalogue and that all of them are passive, we would be able to roughly account for the observed difference.

galaxies is very similar, and only the relative heights change. In what follows, we will therefore simply concentrate on the passive fractions for the central galaxies.

6.2 Modification 1

In our modification 1), we strip the diffuse gas at the same rate as the dark matter of subhaloes is stripped due to tidal effects. We find that the overproduction of passive central galaxies get slightly worse (see Fig. 8, solid cyan lines). The reason for this is that less hot gas is now available for cooling to the central galaxies. For the satellite galaxies, results are improved with respect to DLB07 in the two lower mass bins, while results are similar in the two higher mass bins (see Fig. 9, solid cyan lines). In Fig. 11, cyan lines indicate the distribution of SSFRs for satellite galaxies.

For illustration, we compare the star formation, dark matter and gas accretion histories of two random satellite galaxies at $z=0$ with $\log(M_{\text{star}}/h^{-1}M_{\odot}) \sim 10$. Results are shown for the DLB07 prescriptions (top panels) and for modification 1) (bottom panels) in Fig. 6. In the left hand (right hand) panels, the galaxy becomes a satellite at around a lookback time of 3 Gyr (9 Gyr), which causes the hot and ejected gas reservoir to fall to zero in DLB07. In our modification 1), stripping is much slower. Despite the fact that we always strip the ejected gas first, the hot gas reservoir is depleted more quickly for the galaxy in the right hand panel. This is due to the fact that nearly all hot gas that is added by SN feedback or that is re-incorporated from the ejected phase cools down efficiently in low mass galaxies.

In Fig. 7, we show the relation between the median SSFR and the fraction of the dark matter subhalo mass stripped since infall (top panel), and the lookback time to infall (bottom panel) in modification 1) for galaxies with stellar masses $\log(M/h^{-1}M_{\odot}) = 10 - 10.5$. It can be seen that galaxies typically only become passive after around 80 % of the dark matter subhalo (and thus of the diffuse gas) has been stripped, and only after around 5 Gyr since infall.

6.3 Modification 2 and 2b

We try to address the overproduction of passive central galaxies caused by modification 1) by lowering κ_{AGN} , as defined in eq. 9. Green dot-long dashed lines in Fig. 8 show the effect of modification 2b), in which κ_{AGN} is lowered by a factor of 5. The satellite stripping is treated exactly as in model 1). While results are improved at the massive end, the passive fractions fall well below the observations at intermediate stellar masses. After some experimenting, we found that this problem can largely be solved if satellite galaxies in host haloes with masses below $10^{12}h^{-1}M_{\odot}$ keep all their hot and ejected gas. The reason is that this substantially reduces the amount of gas available for cooling to the central galaxy in such haloes. We implement this change in our modification 2), shown as green dashed lines in Fig. 8. Agreement with observations is improved compared to DLB07, although it is still not perfect.

Why should gas stripping cease to be effective in halos with masses below $10^{12}h^{-1}M_{\odot}$? One reason is that a hot gas halos no longer form at these halo masses (see Fig. 5), which means that ram-pressure stripping will no longer be effective. Our results are in agreement with McGee et al. (2009),

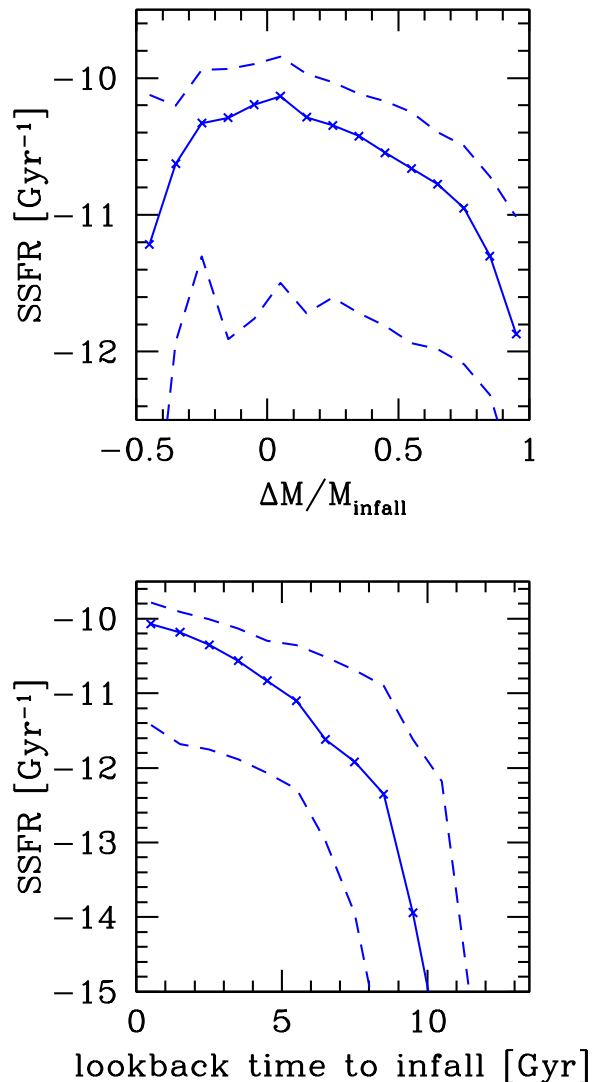


Figure 7. We show the median SSFR and the region where 68 % of the values lie, as a function both of the fraction of mass which has been stripped since infall (top panel) and as a function of the lookback time to the last time the galaxy became a satellite (bottom panel). Results here are shown for galaxies with masses of $\log(M/h^{-1}M_{\odot})=10-10.5$, at $z=0$, in our modification 1).

who find that observations are best reproduced under the assumption that no significant quenching of star formation occurs in host haloes with masses below $\sim 10^{12}h^{-1}M_{\odot}$. We note that significant dark matter stripping does still occur in halos with masses below $10^{12}h^{-1}M_{\odot}$. Our results should thus be taken as an indication that the prescription for gas stripping that we have introduced, in which the gas is removed at the same rate as the surrounding halo loses mass, is simply an *approximation* that appears to give roughly the right answer for satellite galaxies in massive halos. It should not be regarded as a correct representation of the physics that controls the stripping of the gas.

Modification 2) is quite successful in reproducing passive fractions as a function of cluster-centric radius (see Fig. 9, green long-dashed lines). The remaining disagreement is caused by the fact that massive central galaxies are still slightly too passive in this model – this problem propagates

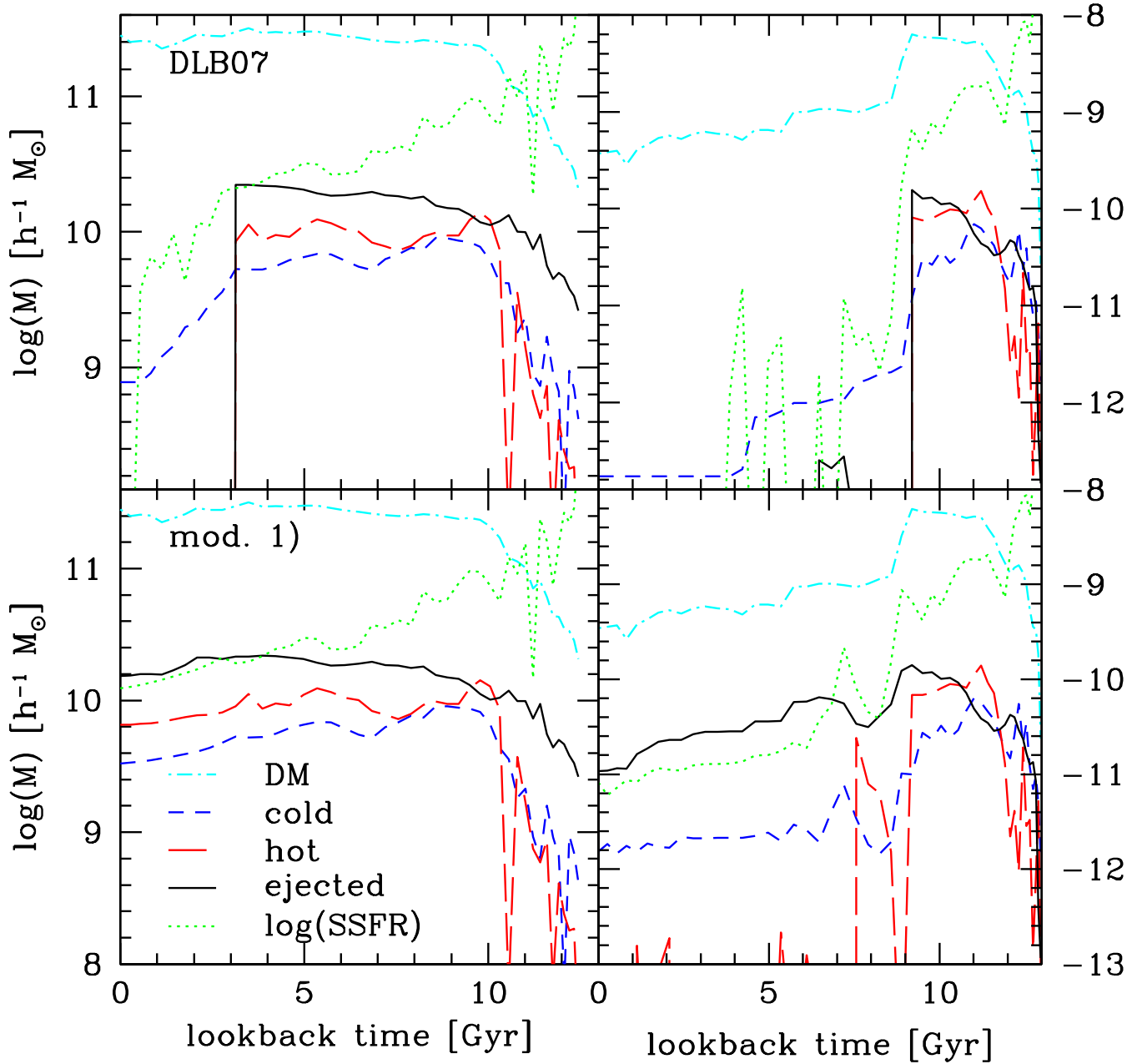


Figure 6. Here we show the histories of two random galaxies with $\log(M_{\text{star}}/h^{-1}M_{\odot}) \sim 10$, for the DLB07 model (top panels) and in our modification 1) (bottom panels). We plot the masses in cold, hot and ejected gas and of the DM subhalo, and $\log(\text{SSFR})$ (with values of the latter given at the right axis of the right hand plots). For both example galaxies, the hot and ejected gas mass drops to zero after infall in DLB07, which happens around 3 Gyr before present in the galaxy shown in the left hand panels, and at around 9 Gyr before present in the galaxy shown in the right hand panels. The galaxy in the right hand panel shortly becomes a central again at around 7 Gyr. At $z=0$, the galaxy in the left hand panel has a stellar mass of $\log(M/h^{-1}M_{\odot})=10.1$ (10.07) in our modification 1) (in DLB07). The galaxy on the right hand panel has a mass of $\log(M/h^{-1}M_{\odot})$ 10.18 (10.09).

to the satellite galaxies irrespective of the stripping that we implement. However, if we look at the detailed distribution of the SSFR of satellite galaxies (Fig. 11, green histogram), we find that the star forming peak of the satellite galaxies is somewhat too low, and that that there are too many satellite galaxies with intermediate SSFR present.

6.4 Modification 3

In modification 3), we correct for fluctuations in subhalo masses, by letting satellite galaxies “accrete” gas from the hot gas reservoir of their host halos, if their dark matter subhalo experiences apparent mass growth. While we find that the distribution of SSFR of satellites is now better reproduced (Fig. 11, red histogram), the passive fractions (Fig. 9, red dashed lines) do not agree as well with the data.

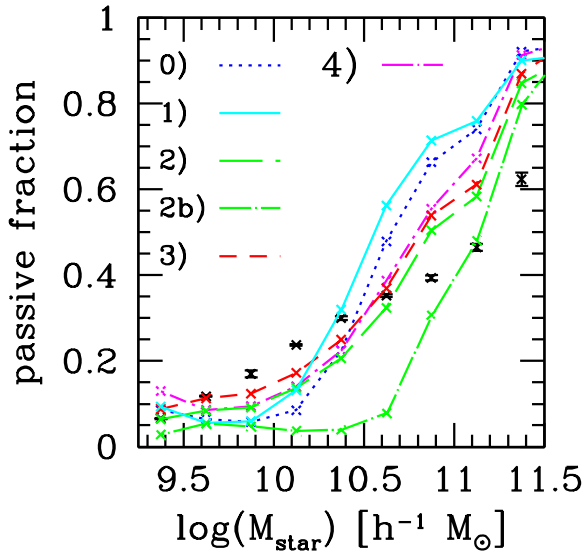


Figure 8. Here we show the impact of our different modifications to the SAM on the passive fraction of central galaxies. Different linestyles correspond to different modifications, as indicated and described in the text. Crosses with errorbars show the observational results.

6.5 Modification 4

By construction, modification 4) produces results that are in good agreement with observations, both in terms of the distribution of SSFR and the passive fractions as a function of cluster-centric radius. The results are shown in Fig. 8 – 11 as magenta dot-dashed lines. Note that it is not possible to obtain a similar level of agreement if we assume that gas is stripped exponentially. While it is relatively easy to reproduce passive fractions, we find that an exponential decline of the gas reservoir cannot at the same time produce a bimodal SSFR distribution for the satellites. Also Balogh et al. (2009) have pointed out that reproducing the detailed bimodal colour distribution of satellite galaxies with SAMs is not trivial.

6.6 The impact on the global properties of the galaxy population

In this section, we investigate the properties of the global galaxy population in our alternative models. We have not tuned our models to match these and it would thus not be surprising if the models were not to agree with the observations. Here, the full simulation box is used. Note that for all results shown here, there is no visible difference between DLB07 and our model 0).

The stellar mass functions in the different models are compared to the observations of Li & White (2009), corrected according to Guo et al. (2009), in the top panel of Fig. 12. All models overproduce the massive end of the stellar mass function. In our models 2) - 4), this problem is accentuated. This is due to the decreased efficiency of AGN feedback that we need in order to reproduce the fraction of passive central galaxies. This clearly indicates that simply decreasing AGN feedback is not a viable solution; maybe, it would be more appropriate to make AGN feedback more stochastic, for example by shutting down gas cooling after

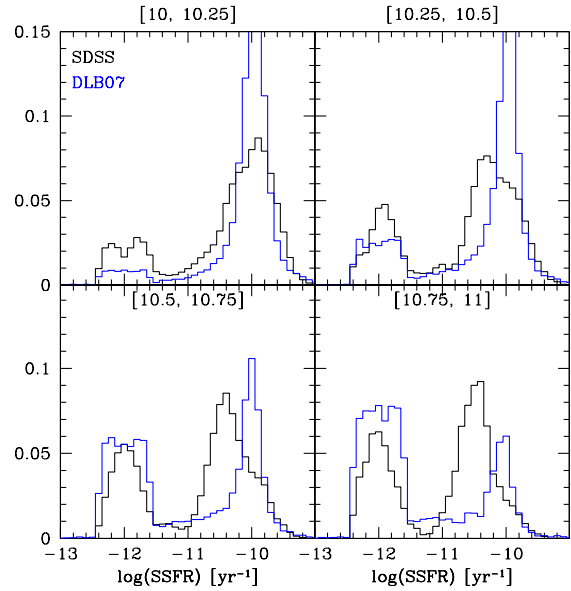


Figure 10. The distribution of the central SSFR in DLB07 compared to the SDSS central galaxies according to Yang et al. (2007). Galaxies with zero SSFR in the SAM are randomly distributed between $\log(\text{SSFR})=-11.6$ and $\log(\text{SSFR})=-12.4$, and the same is done for SDSS galaxies with measured $\log(\text{SSFR}) < -12.4$. Results for our alternative SAMs are not shown since the location of the peak is identical with DLB07, and only the relative peak heights change, which is information already given in Fig. 8.

major mergers (e.g. Hopkins et al. 2008). Interestingly, the overproduction of luminous galaxies is more severe in our modification 3) than in our modification 2), which only differ in details of the implementation of satellite gas stripping. This indicates that the treatment of satellite can have a significant impact on the general galaxy population.

In Fig. 13, we compare the total b_J -band luminosity function (LF hereafter, top panel) and the red b_J -band LF (bottom panel) for the different models to observations. Galaxies are classified as red if $B - V < 0.8$, following Croton et al. (2006). Observations are taken from Norberg et al. (2002) and Madgwick et al. (2002). Again, the impact of decreasing AGN feedback in our modifications 2) - 4) is clearly apparent. In the bottom panel of Fig. 13, it can be seen that all models shown here have some problems with reproducing the red LF. Interestingly, our improved treatment of satellite stripping does not entirely solve the overproduction of faint red galaxies noted by Croton et al. (2006). We note that our ability to link gas stripping to the evolution of the dark matter mass of the subhalo will break down near the resolution limit of the simulation. Right now we assume that all the gas is stripped when the subhalo is finally disrupted. This will likely result in effective gas stripping efficiencies that are too high for the low mass satellites. It thus might be advisable to use a different method for galaxies that reside in subhalos with masses at infall close to the resolution limit. One possibility is to adopt modification 4) in this regime. Indeed, Figure 11 shows that modification 4) gives improved agreement with the faint end of the red LF.

Another problem becomes apparent at intermediate luminosities in our modifications 2) - 4), where the number of red galaxies is too low. This may be related to the decrease

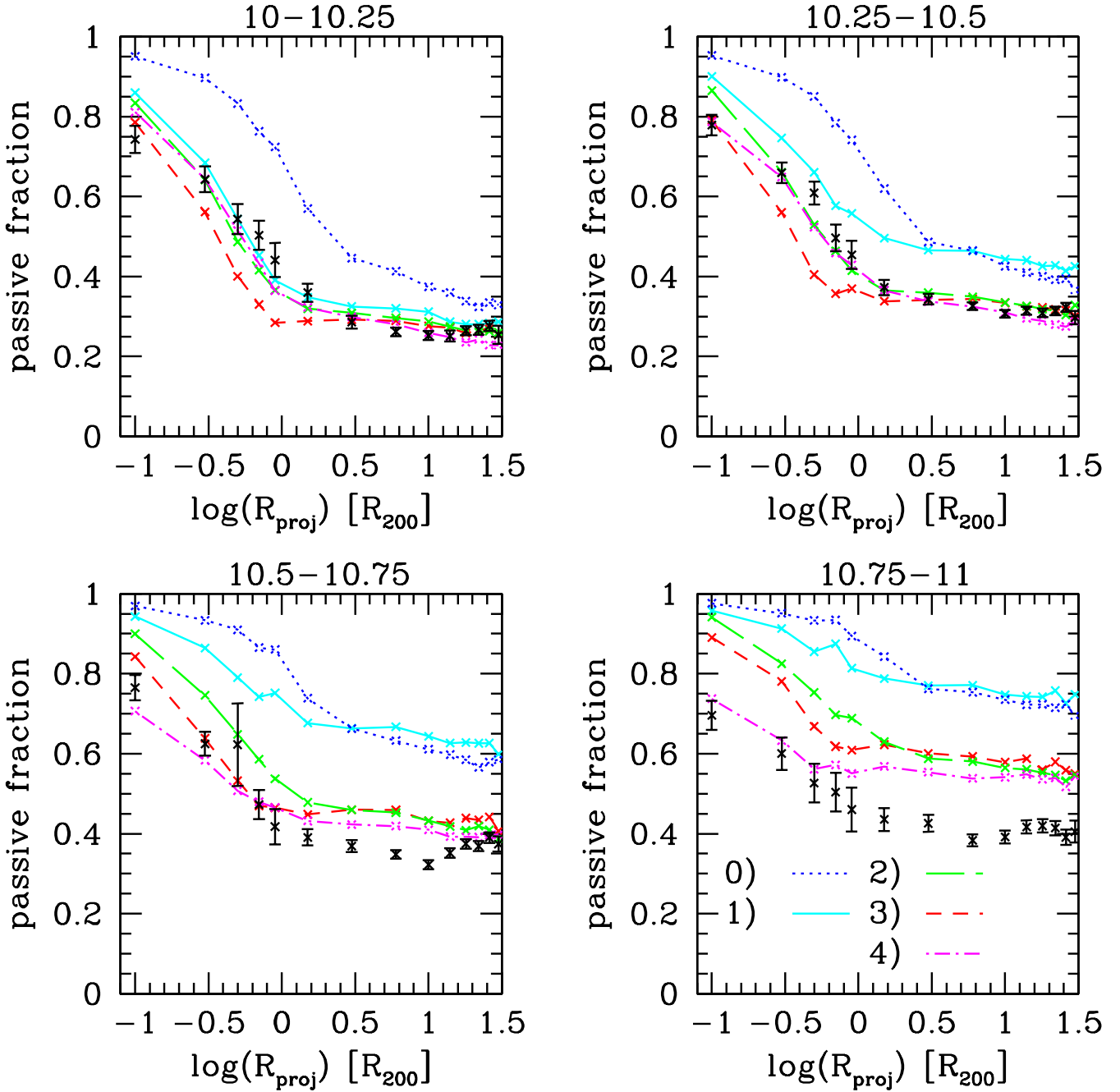


Figure 9. Here we show the impact on our modifications on the passive fraction as a function of cluster-centric radius in four different stellar mass bins, as indicated on the top of the panel. Different line styles correspond to four alternative SAMs, as indicated and described in the text. Crosses with errorbars show the observational results. Only clusters with masses above $10^{14}h^{-1}M_{\odot}$ are used.

in AGN feedback. Stronger dust attenuation in these galaxies may solve this problem, but we do not investigate this issue in more detail here.

Our results show that the implementation of the stripping of the satellite galaxy gas supply in proportion to the dark matter does not impact the global properties of galaxies very significantly, except by decreasing the abundances of faint red galaxies to some degree. However, decreasing the AGN feedback, and shutting off satellite stripping at halo masses below $10^{12}h^{-1}M_{\odot}$ in order to better reproduce the passive fraction of central galaxies clearly leads to inconsis-

tencies with the LF. It is likely that in order to simultaneously reproduce the passive fraction of centrals, the LF of red galaxies and the bright end of the LF, a more careful retuning of the model, including the prescriptions for AGN feedback and dust attenuation, will have to be carried out.

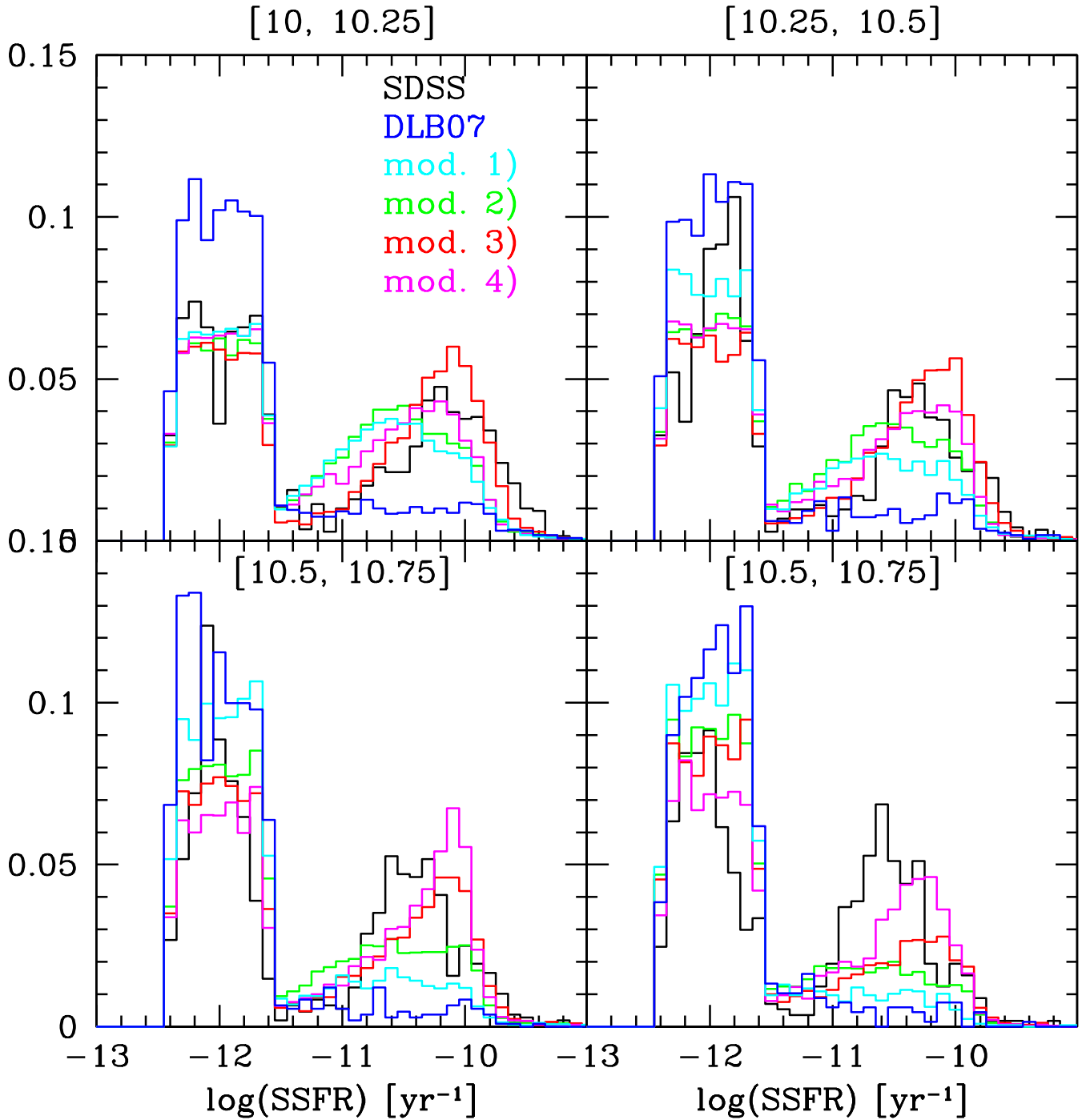


Figure 11. The distribution of the satellite SSFR in DLB07 and our 4 modifications compared to observed satellite SSFRs. Galaxies with zero SSFR in the SAM are randomly distributed between $\log(\text{SSFR})=-11.6$ and $\log(\text{SSFR})=-12.4$, and the same is done for SDSS galaxies with measured $\log(\text{SSFR}) < -12.4$. Both in the models and the observations, satellite galaxies are defined as galaxies residing within R_{200} from the centers of clusters with masses $> 10^{14} h^{-1} M_{\odot}$ as found by the bi-weight algorithm described in section 2.4.

7 DISCUSSION

7.1 Treatment of satellite galaxies in the SAM

Recently, several observational and theoretical studies have shown that the removal of the gas reservoir in satellite galaxies is overly efficient in most current SAMs (McCarthy et al. 2008; Simha et al. 2008; Font et al. 2008; Weinmann et al.

2006b; Wang et al. 2007). In this work, we present a simple way to treat environmental effects.

It seems physically plausible that the stripping efficiency may depend on the mass of the host halo, on the mass of the satellite galaxy (e.g. Bekki 2009), on orbital parameters (e.g. McCarthy et al. 2008) and on the age of the Universe (e.g. Giocoli et al. 2008). These dependencies, however, are not well constrained. It is not clear whether

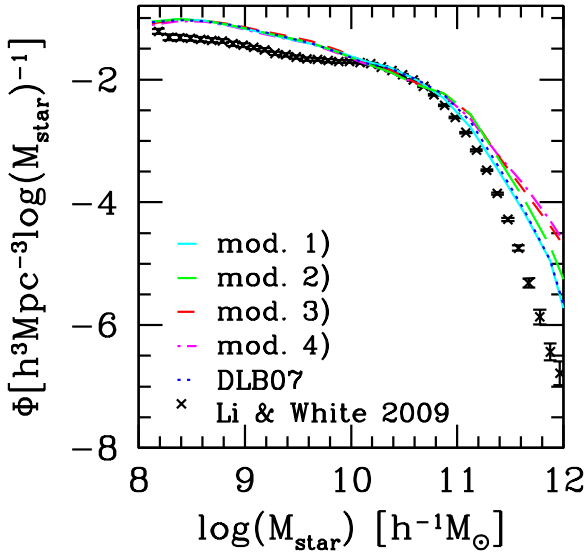


Figure 12. The stellar mass functions in the standard model of DLB07 (blue dotted lines) and in our modifications of this model, as indicated. The observed mass function is a modified version of the one presented in Li & White (2009), corrected according to Guo et al. (2009).

hydrodynamical simulations can properly predict the distribution of the (probably multiphase) hot and ejected gas, or deal with the presence of shielding magnetic fields. Smooth particle hydrodynamics codes may have difficulties dealing with dynamical instabilities occurring in regions with steep gas density gradients (e.g. Agertz et al. 2007).

In this work, we suggest using the approximation that the diffuse gas halo of the satellite (which includes the hot and ejected gas) is stripped at the same rate as the dark matter halo. This is a very simple model which does not treat the detailed physics of gas stripping, but is easy to implement. We find that observations at $z=0$ can also be well reproduced by a simple recipe in which 10-20 % of the initial gas reservoir in the halo is stripped per Gyr. We stress that in order to reproduce observations, the diffuse gas must be stripped linearly, and not exponentially.

It is not yet clear whether environmental effects at higher redshift are correctly reproduced by this method. We find that the dark matter stripping seems to be more efficient at high redshift than at $z=0$. It will be a natural next step to compare our models to observations of galaxy properties as a function of environment at higher redshifts.

Eventually, it will be important to understand the nature of the gas that is found around satellite galaxies. “Starvation” is usually defined as the stripping of the hot gas halo (Larson, Tinsley & Caldwell 1980). However, below a mass limit of around $10^{12} h^{-1} M_{\odot}$, gas cools rapidly and thus does not stay in a hot gas reservoir for a significant amount of time. Consequently, most gas in low mass haloes resides in the so-called “ejected”, and not in the “hot phase”, with the ejected mode composed of gas that has been expelled from the galaxy by supernovae. The state of this ejected gas is very poorly understood: it could consist of cold clumps, or it might form an extended disk, or it might have high temperatures and low densities. The only certainty we have about this phase is that it must remain bound to the galaxy

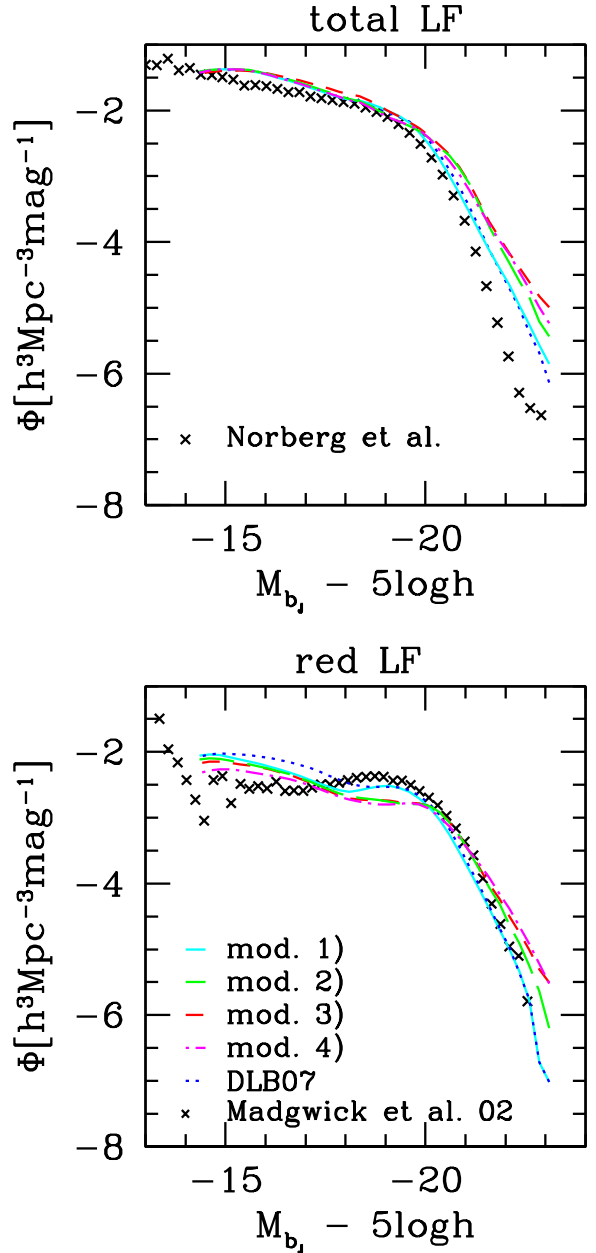


Figure 13. The total b_J -band luminosity function (top panel) and the b_J -luminosity function of red galaxies alone (bottom panel) for the standard model of DLB07 (blue dotted lines) and our modifications of this model, as indicated. Observations are taken from Norberg et al. (2002) and Madgwick et al. (2002) and are shown as crosses and without errorbars. The split into blue and red galaxies has been done at $B - V = 0.8$.

and form a significant part of the reservoir for future star formation in low mass systems. At low stellar masses, stripping of this ejected phase is the main driver of environmental effects in the local Universe.

In this work, we have not considered the abundances of satellite galaxies as a function of halo mass or the correlation function on small scales; in order to reproduce these observations, it is likely that tidal disruption and satellite-satellite mergers have to be taken into account, as SAMs tend to overproduce the abundance of satellite galaxies (e.g. Liu et

al. 2009). Tidal disruption might also help with reproducing the bright end of the luminosity function, as the number of mergers would be reduced, and would explain the presence of significant intracluster light (Zibetti et al. 2005). Suggestions of how tidal stripping might be implemented into SAM can be found in Kim et al. (2009), Wetzel & White (2009) and Henriques & Thomas (2009). Also, we have not considered the stellar ages and metallicities of satellites, for which Pasquali et al. (2009b) have found some interesting discrepancies between SAMs and observations. These may help to further constrain the physics of satellite stripping in future work.

7.2 Comparison to a simple model of ram-pressure stripping

Gunn & Gott (1972) were the first to suggest that the ram pressure of the hot intracluster medium may strip gas from galaxies. Ram-pressure stripping of the *cold* disk gas has since received considerable theoretical attention (e.g. Abadi et al. 1999; Schulz & Struck 2001; Roediger & Brüggen 2007). Ram-pressure stripping of the hot gas halo, however, has been investigated by only a few studies (e.g. Mori & Burkert 2000; Hester 2006; McCarthy et al. 2008). McCarthy et al. (2008) find that ram-pressure stripping is more efficient than tidal stripping in depleting the hot gas halo of most satellite galaxies. Our simple prescription described in section 5 does not explicitly model this effect. In this section, we test whether we can reproduce observations by implementing ram-pressure stripping in a physically motivated fashion.

Our model is based on the model of ram-pressure stripping by Font et al. (2008), but with a few important modifications. We follow the orbits of the satellites in detail, and allow stripping at every timestep, while Font et al. (2008) only allow stripping at infall and at each time the host halo doubles in mass. We assume that the ram-pressure stripping of the hot gas proceeds from the outside in, and does not affect the central density and hence the cooling efficiency of the satellite hot gas³. We allow the assumption of outside-in stripping to break down if the truncation radius of the hot halo reaches some fraction β of the virial radius of the dark matter halo that hosts the satellite at the time of infall. At this point, we allow the density profile of the hot gas to relax to an isothermal distribution out to the virial radius R_{vir} , and we strip all the ejected gas.

We describe the detailed implementation of the model in the L-galaxies code. While $R_{\text{trunc}} > \beta R_{\text{vir}}$, we describe the density profile of the hot gas for satellites with a modified version of eq. 6, following Font et al. (2008):

$$\rho_g(r) = \begin{cases} \frac{m_{\text{hot}} + m_{\text{strip}}}{4\pi R_{\text{vir}} r^2} & \text{if } r < R_{\text{trunc}} \\ 0 & \text{if } r > R_{\text{trunc}} \end{cases} \quad (16)$$

where m_{strip} is the sum of all hot gas which has been stripped from the galaxy since it became a satellite. R_{trunc} is set to R_{vir} when a galaxy first changes from central to satellite.

³ Unlike Font et al. (2008), we do not limit the cooling radius (r_{cool} , see eq. 4 and 5) by R_{trunc} . In eq. 4, we replace m_{hot} by $m_{\text{hot}} + m_{\text{strip}}$ for satellite galaxies.

(Note that R_{vir} and V_{vir} for satellites are fixed at infall and then remain constant.)

The stripping radius R_{strip} is calculated according to Gunn & Gott (1972) and McCarthy et al. (2008) as the radius where the ram pressure exceeds the pressure induced by the self-gravity of the satellite. For a singular isothermal sphere of hot gas, we determine R_{strip} with

$$\alpha \rho_{g,\text{sat}}(R_{\text{strip}}) V_{\text{vir,sat}}^2 = \rho_{g,\text{cen}}(R) V^2 \quad (17)$$

with R and V indicating the distance of the satellite to the cluster center, and its velocity relative to it. For the pressure exerted by the self-gravity of the satellite, we use a prefactor $\alpha = 2$, following McCarthy et al. (2008). However, we note that removing this prefactor has very little impact on the results. If $R_{\text{strip}} < R_{\text{trunc}}$, we remove all the mass enclosed between those two radii, and set $R_{\text{trunc}} = R_{\text{strip}}$.

If $R_{\text{trunc}} < \beta R_{\text{vir}}$, we reset $m_{\text{strip}} = 0$ and $R_{\text{trunc}} = R_{\text{vir}}$, which means that the hot gas gets diluted out to R_{vir} , leading to strongly decreased cooling, and increased vulnerability to stripping. Galaxies often fluctuate between the central and satellite status. Whenever a satellite galaxy becomes a central again, its R_{vir} is updated according to its current dark matter subhalo. R_{trunc} is set to R_{vir} . After each stripping event, the hot gas mass in the satellite will be modified by cooling, ejection, SN feedback and reincorporation. Before we calculate the stripping occurring in the next timestep, we reset the truncation radius such that

$$M(r < R_{\text{trunc}}) = M_{\text{hot}}. \quad (18)$$

Up to now, we have only discussed the ram-pressure stripping of the hot gas component. As shown in Fig. 5, the ejected gas mass exceeds the hot gas mass in low mass galaxies, and it is thus of crucial importance how its stripping is modelled. Here, we follow Font et al. (2008) and simply assume that in a given stripping event, the stripped fraction of ejected gas equals the stripped fraction of hot gas. If $R_{\text{trunc}} < \beta R_{\text{vir}}$, we assume that all the ejected gas is stripped.

We now implement the above model into a SAM based on DLB07, which includes the first three modifications in section 5.2. No tidal stripping is included, and the AGN feedback efficiency is set to be the same as in DLB07 for easier comparison. We compare two different models: R1) and R2). In model R1), we use $\beta = 0.1$, and in model R2), $\beta = 0.01$. Results for the stellar mass bins $\log(M/h^{-1}M_{\odot}) = 10-10.25$ (top panel) and $\log(M/h^{-1}M_{\odot}) = 10.5-10.75$ (bottom panel) are shown as green dashed lines for model R1) and as magenta dot-dashed lines for model R2) in Fig. 14. For comparison, we also show results from DLB07 and our model 1), where the diffuse gas is stripped at the same rate as the dark matter.

For low mass galaxies, we find that the ram-pressure is much more efficient at stripping out the gas than model 1), and both models R1) and R2) produce passive fractions that are too high to match observations.⁴ On the other hand,

⁴ We have also tested a model with $\beta=0$, which means that the central density of the hot gas is never affected by stripping. In this case, satellite galaxies have as high star formation rates as central galaxies. Interestingly, this indicates that it is not the reduced hot gas mass, but the reduced central density of the hot gas, which causes environmental effects in all our models.

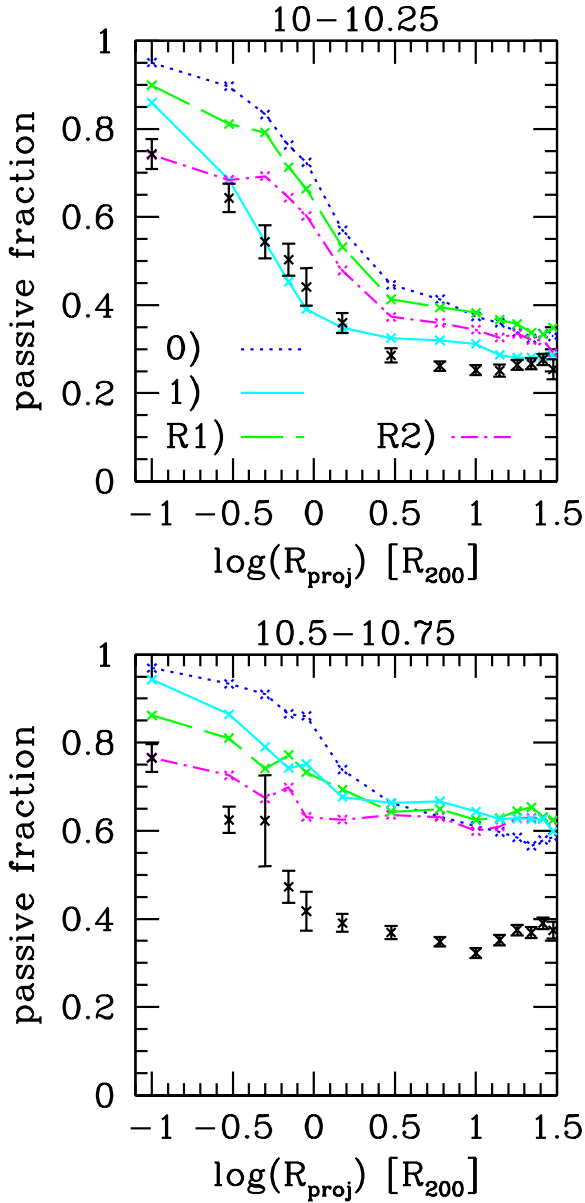


Figure 14. Passive fraction as a function of cluster-centric radius at stellar masses of $\log(M/h^{-1}M_{\odot})=10 - 10.25$ (top panel) and $10.5 - 10.75$ (bottom panel). Different line styles and colours correspond to DLB07 (blue dotted lines), our model 1) (cyan solid lines) and the two models R1) and R2) including ram-pressure stripping and no tidal stripping (green dashed lines and magenta dot-dashed lines) as indicated and described in the text. Crosses with errorbars show the observational results. Only clusters with masses above $10^{14}h^{-1}M_{\odot}$ are used.

in high mass galaxies, the ram-pressure effects are weaker than the tidal effects, and the ram-pressure models cannot produce a strong enough change in passive fraction as a function of clustercentric radius. In Fig. 15, we show the distribution of SSFR for the stellar mass bin $\log(M/h^{-1}M_{\odot}) = 10-10.25$. In magenta, we show results for the model R2). Clearly, there are too many galaxies with intermediate SSFR in this model.

In summary, we find three problems with a model in which environmental effects arise solely due to ram-pressure

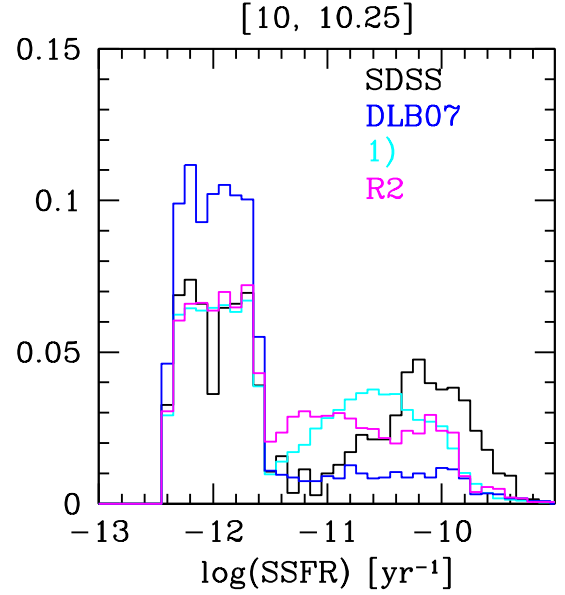


Figure 15. The distribution of satellite SSFR at stellar masses of $\log(M/h^{-1}M_{\odot})=10 - 10.25$. Different colours correspond to DLB07 (blue lines), our model 1) (cyan lines) and the ram-pressure stripping model R2) as indicated and described in the text. Black lines show the observational results. Only clusters with masses above $10^{14}h^{-1}M_{\odot}$ are used.

stripping. First, stripping effects in clusters for low mass galaxies are too strong to explain the observations. Second, stripping effects are not strong enough to reproduce the observations for high mass galaxies. Third, there are too many low mass galaxies with intermediate SSFR. The first problem could indicate that our understanding of the so-called “ejected phase”, which is important for low mass galaxies, is inaccurate. Although the ejected gas is currently unavailable for star formation, it maybe nevertheless strongly bound to the galaxy, and difficult to strip. Another potential reason for the problem is that SAMs like DLB07 are likely to overestimate the hot gas mass in groups with masses between 10^{12} and $10^{14}h^{-1}M_{\odot}$, especially in the central, most dense regions of these systems (Bower et al. 2008). This could lead to too strong pre-processing of cluster galaxies in groups. The second problem could indicate that tidal effects are in fact important for higher mass galaxies. By decreasing the dark matter content in subhaloes, tidal effects make high mass galaxies more vulnerable to ram-pressure stripping, but also to AGN feedback. The third problem indicates that ram-pressure stripping as implemented here does not produce a bimodal satellite galaxy population. A similar problem seems to be present in the ram-pressure stripping model of Font et al. (2008), as pointed out by Balogh et al. (2009). This could also hint at the importance of tidal effects, which we have shown to produce bimodal distribution in the SSFR of galaxies.

We note that Font et al. (2008) have found that their ram-pressure model can reproduce the colours of satellite galaxies well. As they do not follow the orbits of individual satellites in detail, and use different assumptions for the hot gas profiles and the treatment of cooling in satellites, it is

hard to directly compare the two models and to pinpoint the reason for this discrepancy.

8 SUMMARY

We explore a set of modifications to the SAM of DLB07 with the goal to reproduce (i) the passive fractions as a function of cluster-centric radius out to the field, (ii) the detailed distribution of the SSFRs of satellite galaxies and (iii) the passive fractions of central galaxies as a function of stellar mass. We apply a realistic cluster finder to the SAM to allow a fair comparison with observational results from the cluster catalogue of vdL07. Our main results are the following.

- A model in which the diffuse gas is stripped at the same rate that the dark matter subhalos lose mass due to tidal stripping can reproduce observations reasonably well. “Starvation” is usually defined as the fast removal of the hot gas halo surrounding satellite galaxies (Larson, Tinsley & Caldwell 1980) due to both tidal and ram-pressure stripping. In this work, we find indications that this picture is in need of revision. First, stripping of the diffuse gas reservoir is slow. Second, it is crucial for the success of our model that even the gas ejected by supernovae is not stripped instantaneously, but viewed as part of the overall gas reservoir.

- After infall, the median subhalo identified at $z=0$ loses 15–20% of its initial dark matter halo mass per Gyr, which implies that tidal stripping is typically only complete after 5–7 Gyrs. Dark matter stripping seems to proceed linearly, and not exponentially. This is crucial for reproducing the observed bimodality in the specific star formation rates of satellites in our model. We also find that stripping of dark matter becomes more efficient at high redshift.

- We present a simple method for implementing gas stripping in SAMs which do not follow the dark matter subhaloes of satellites. Our prescription is that 10–20% of the hot and ejected gas recorded at infall should be stripped per Gyr. This model gives good agreement with observations at $z=0$.

- A model which only includes a physically motivated prescription for ram-pressure stripping of the hot gas in satellite galaxies seems to lead to an overproduction of low mass passive galaxies in clusters, but also too little environmental effects for high mass galaxies.

- We have found that DLB07 do not reproduce the passive fraction of central galaxies as a function of stellar mass in detail. In particular, DLB07 predict too few passive central galaxies with low masses, and too many with high masses. We find that we can improve agreement with observations by reducing the AGN feedback efficiency, and by assuming that satellite galaxies in host haloes with masses below $10^{12}h^{-1}M_{\odot}$ retain all their hot and ejected gas. However, the reduction of AGN feedback leads to an overproduction of the total number of massive and luminous galaxies. In order to simultaneously reproduce the low abundance, and the relatively high active fraction of massive galaxies, the form of the AGN feedback in DLB07 may need to be changed. One possible way to solve this problem might be to introduce some stochasticity into the shut-down of cooling at high halo masses, for example by taking into account the effect of major mergers or morphological quenching (Hopkins et al. 2008; Martig et al. 2009). We also find that reproducing both the red luminosity function and the passive fraction of

central and satellite galaxies is surprisingly difficult, indicating either an inconsistency between different observations, or a potential problem with the dust treatment in the SAM.

ACKNOWLEDGMENTS

SW thanks Eyal Neistein for a careful reading of the manuscript and many helpful comments; Qi Guo, Andreea Font, Simon White, Richard Bower, Barbara Catinella, Andreas Faltenbacher, Ramin Skibba, Yan-Mei Chen, Andrea Macciò and Xi Kang for useful discussion, and Volker Springel and Mike Boylan-Kolchin for their help with the Millennium database. We also thank the anonymous referee for the suggestion to add a model for ram-pressure stripping. GDL acknowledges financial support from the European Research Council under the European Community’s Seventh Framework Programme (FP7/2007-2013)/ERC grant agreement n. 202781.

REFERENCES

- Abadi M., Moore B., Bower R., 1999, MNRAS, 308, 947
 Agertz O., et al., 2007, MNRAS, 380, 963
 Bamford S.P., 2009, MNRAS, 393, 1324
 Baldry I.K., Balogh M.L., Bower R.G., Glazebrook K., Nichol R.C., Bamford S.P., Budavari T., 2006, MNRAS, 373, 469
 Balogh M.L., Morris S.L., Yee H.K.C., Carlberg R.G., Ellingson E., 1997, ApJ, 488, L75
 Balogh M.L., Christlein D., Zabludoff A.I., Zaritsky D., 2001, ApJ, 557, 117
 Balogh M.L. et al., 2009, MNRAS, 398, 754
 Barkhouse W.A., Yee H.K.C., López-Cruz O., 2009, ApJ, 703, 2024
 Beers T.C., Flynn K., Gebhardt K., 1990, AJ, 100, 32
 Bekki K., 2009, MNRAS, 399, 2221
 Best P.N., von der Linden A., Kauffmann G., Heckman T.M., Kaiser C.R., 2007, MNRAS, 379, 894
 Blanton M.R. et al. 2005, AJ, 129, 2562
 Bolzanella M., et al., 2009, preprint (arXiv:0907.0013)
 Bower R.G., McCarthy I.G., Benson A.J., 2008, MNRAS, 390, 1399
 Brinchmann J., Charlot S., White S.D.M., Tremonti C., Kauffmann G., Heckmann T., Brinkmann J., 2004, MNRAS, 351, 1151
 Cole S., Lacey C.G., Baugh C.M., Frenk C.S., 2000, MNRAS, 319, 168
 Croton D.J. et al., 2006, MNRAS, 365, 11
 De Lucia G., Kauffmann G., Springel V., White S.D.M., Lanzoni B., Stoehr F., Tormen G., Yoshida N., 2004, MNRAS, 348, 333
 De Lucia G., Blaizot J., 2007, MNRAS, 375, 2 (DLB07)
 De Lucia G., Helmi A., 2008, MNRAS, 391, 14
 De Propris R. et al., 2004, MNRAS, 351, 125
 Diaferio A., Kauffmann G., Balogh M., White S.D.M., Schade D., Ellingson E., 2001, MNRAS, 323, 999
 Diemand J., Kuhlen M., Madau P., 2007, ApJ, 667, 859
 Dressler A., 1980, ApJ, 236, 351
 Font A.S., et al., 2008, MNRAS, 389, 1619
 Gao L., White S.D.M., Jenkins A., Stoehr F., Springel V., 2004, MNRAS, 355, 819
 Giocoli C., Tormen G., van den Bosch F.C., 2008, MNRAS, 386, 2135
 Goto T., Masafumi Y., Tanaka M., Okamura S., 2004, MNRAS, 348, 515

- Gunn J.E. & Gott J.R.III, 1972, *ApJ*, 176, 1
- Guo Q., White S.D.M., Li C., Boylan-Kolchin M., 2009, arXiv:0909.4305
- Hansen S.M., Sheldon E.S., Wechsler R.H., Koester B.P., 2009, *ApJ*, 699, 1333
- Hayashi E., Navarro J.F., Taylor J., Stadel J., Quinn T., 2003, *ApJ*, 584, 541
- Henriques B.M., Thomas P.A., 2009, preprint (arXiv:0909.2150)
- Hester J.A., 2006, *ApJ*, 647, 910
- Hopkins P.F., Cox T.J., Kereš D., Hernquist L., 2008, *ApJ*, 175, 390
- Kang X., Jing Y.P., Silk J., 2006, *ApJ*, 648, 820
- Kang X., van den Bosch F.C., 2008, *ApJ*, 676, 101
- Kauffmann G., White S.D.M., Guideroni B., 1993, *MNRAS*, 264, 201
- Kauffmann G., 1996, *MNRAS*, 281, 475
- Kauffmann G. et al., 2003, *MNRAS*, 341, 33
- Kazantzidis S., Mayer L., Mastropietro C., Diemand J., Stadel J., Moore B., 2004, *ApJ*, 608, 663
- Kennicutt R.C., 1998, *ApJ*, 498, 576
- Kim H.S., Baugh C.M., Cole S., Frenk C.S., Benson A.J., 2009, preprint, (arXiv:0905.4723)
- Kimm T. et al., 2009, *MNRAS*, 394, 1131
- Koester B.P., et al., 2007, *ApJ*, 660, 239
- Lanzoni B., Guideroni B., Mamon G.A., Devriendt J., Hatton S., 2005, *MNRAS*, 361, 369
- Larson R.B., Tinsley B.M., Caldwell C.N., 1980, *ApJ*, 237, 692
- Li C., White S.D.M., 2009, *MNRAS*, 398, 2177
- Liu L., Yang X., Mo H.J., van den Bosch F.C., Springel V., 2009, preprint (arXiv:0912.1257)
- Limousin M., Kneib J.P., Bardeau S., Natarajan P., Czoske O., Smail I., Ebeling H., Smith G.P., 2007, *A&A*, 461, 881
- Maciejewski M., Colombi S., Springel V., Alard C., Bouchet F.R., 2009, *MNRAS*, 396, 1329
- Madgwick D.S., 2002, *MNRAS*, 333, 133
- Martig M. Bournaud F., Teyssier R., Dekel A., 2009, *ApJ*, 707, 250
- Martin C.L., 1999, *ApJ*, 513, 156
- Martínez H.J., O'Mill A.L., Lambas D.G., 2006, *MNRAS*, 372, 253
- McCarthy I.G. et al., 2008, *MNRAS*, 383, 593
- McGee S.L., Balogh M.L., Bower R.G., Font A.S., McCarthy I.G., 2009, *MNRAS*, 400, 937
- Miller C.J. et al., 2005, *ApJ*, 130, 968
- Mo H.J., Mao S., White S.D.M., 1998, *MNRAS*, 295, 319
- Mori M., Burkert A., 2000, *ApJ*, 538, 559
- Natarajan P., De Lucia G., Springel V., 2007, *MNRAS*, 376, 180
- Natarajan P., Kneib J.P., Smail I., Treu T., Ellis R., Moran S., Limousin M., Czoske O., 2009, *ApJ*, 693, 970
- Neistein E., Weinmann S.M., 2009, preprint (arXiv:0911.3147)
- Norberg P. et al., 2002, *MNRAS*, 336, 907
- Oemler A., 1974, *ApJ*, 194, 1
- Okamoto T., Nagashima M., 2003, *ApJ*, 587, 500
- Oppenheimer B.D., Davé R., Kereš D., Fardal M., Katz N., Kollmeier J.A., Weinberg D.H., 2009, arXiv:0912.0519
- Pasquali A., van den Bosch F.C., Mo H.J., Yang X., Somerville R., 2009a, *MNRAS*, 394, 38
- Pasquali A., Gallazzi A., Fontanot F., van den Bosch F.C., De Lucia G., Mo H.J., Yang X., 2009b, arXiv:0912.1853
- Postman M., Geller M.J., 1984, *ApJ*, 281, 95
- Roediger E., Brüggén M., 2007, *MNRAS*, 380, 1399
- Salim S. et al., 2007, *ApJ*, 173, 267
- Schimminovich D. et al., 2007, *ApJ*, 173, 315
- Schulz S., Struck C., 2001, *MNRAS*, 328, 185
- Simha V., Weinberg D.H., Davé R., Gnedin O.Y., Katz N., Kereš D., 2009, *MNRAS*, 399, 650
- Somerville R.S., Hopkins P.F., Thomas J.C., Robertson B.E., Hernquist L., 2008, *MNRAS*, 391, 481
- Spergel D.N., Verde L., Peiris H.V., et al., 2003, *ApJ*, 148, 175
- Springel V., White S.D.M., Tormen G., Kauffmann G., 2001, *MNRAS*, 328, 726
- Springel V. et al., 2005, *Nature*, 435, 629
- Sutherland R.S., Dopita M.A., 1993, *ApJ*, 88, 253
- Tanaka M., Goto T., Okamura S., Shimasaku K., Brinkmann J., 2004, *AJ*, 128, 2677
- Taylor J.E., Babul A., 2001, *ApJ*, 559, 716
- Tinker J.L., Wetzel A., 2009, preprint (arXiv:0909.1325)
- van den Bosch F.C., Pasquali A., Yang X., Mo H.J., Weinmann S., McIntosh D.H., Aquino D., 2008, preprint (arXiv:0805.0002)
- van den Bergh S., 2000, *The galaxies of the Local Group*, Cambridge University Press
- von der Linden A., Best P.N., Kauffmann G., White S.D.M., 2007, *MNRAS*, 379, 894 (vdL07)
- von der Linden A., Wild V., Kauffmann G., White S.D.M., Weinmann S.M., 2009, preprint (arXiv:0909.3522)
- Wang L., Li C., Kauffmann G., De Lucia G., 2007, *MNRAS*, 377, 1419
- Weinmann S.M., van den Bosch F.C., Yang X., Mo H.J., 2006a, *MNRAS*, 366, 2
- Weinmann S.M., van den Bosch F.C., Yang X., Mo H.J., Croton D.J., Moore B. 2006b, *MNRAS*, 372, 1161
- Wetzel A.R., White M., 2009, preprint (arXiv:0907.0702)
- Yang X., Mo H.J., van den Bosch F.C., Pasquali A., Li C., Barden M., 2007, *ApJ*, 671, 153
- Yang X., Mo H.J., van den Bosch F.C., Jing Y.P., 2005, *MNRAS*, 356, 1293
- Zentner, A.R., Berlind A.A., Bullock J.S., Kravtsov A.V., Wechsler R. H., 2005, *ApJ*, 624, 505
- Zibetti S., White S.D.M., Schneider D.P., Brinkmann J., 2005, *MNRAS*, 358, 949